

Article

Jeans Instability of Dissipative Self-Gravitating Bose–Einstein Condensates with Repulsive or Attractive Self-Interaction: Application to Dark Matter

Pierre-Henri Chavanis

Laboratoire de Physique Théorique, Université de Toulouse, CNRS, UPS, 31062 Toulouse, France; chavanis@irsamc.ups-tlse.fr

Received: 13 October 2020; Accepted: 15 November 2020; Published: 27 November 2020



Abstract: We study the Jeans instability of an infinite homogeneous dissipative self-gravitating Bose–Einstein condensate described by generalized Gross–Pitaevskii–Poisson equations [Chavanis, P.H. *Eur. Phys. J. Plus* **2017**, *132*, 248]. This problem has applications in relation to the formation of dark matter halos in cosmology. We consider the case of a static and an expanding universe. We take into account an arbitrary form of repulsive or attractive self-interaction between the bosons (an attractive self-interaction being particularly relevant for the axion). We consider both gravitational and hydrodynamical (tachyonic) instabilities and determine the maximum growth rate of the instability and the corresponding wave number. We study how they depend on the scattering length of the bosons (or more generally on the squared speed of sound) and on the friction coefficient. Previously obtained results (notably in the dissipationless case) are recovered in particular limits of our study.

Keywords: Jeans instability; self-gravitating Bose-Einstein condensates; dark matter

1. Introduction

Cosmological observations have revealed that baryonic (visible) matter represents only 5% of the content of the Universe. The rest of the Universe is invisible, being made of 25% dark matter (DM) and 70% dark energy (DE) [1]. DE has been introduced to explain why the expansion of the universe is presently accelerating. This may be due to a nonvanishing value of the Einstein cosmological constant [2], to a scalar field (SF) rolling down a potential like quintessence [3], or to an exotic fluid with a negative pressure like the Chaplygin gas [4]. DM has been introduced to explain why the rotation curves of disk galaxies tend to a plateau at large distances with a constant rotational velocity $v_\infty \sim 200$ km/s [5] instead of declining according to the Keplerian law like for the rotation of the planets around the sun (the rotation curves go up to 50 kpc while the mass of visible matter converges within ~ 10 kpc).¹ Although some authors like Milgrom [7] have proposed an explanation of the flat rotation curves of the galaxies in terms of a theory of modified gravity (MOND) without the need for DM, the most likely scenario is to assume that galaxies are surrounded by DM halos whose mass $M(r) \sim v_\infty^2 r / G$ increases linearly with the distance so that the rotational velocity $v(r) = \sqrt{GM(r)/r} \rightarrow v_\infty$. This is the case if DM halos can be modeled as an isothermal gas with an effective temperature $k_B T / m = v_\infty^2 / 2$. In that case, their density decreases as $k_B T / (2\pi G m r^2)$ at large distances yielding flat rotation curves [8].

¹ The first hints about the existence of a large amount of invisible matter in the universe date back to Zwicky [6] in 1933. He applied the virial theorem to the Coma cluster and found that some mass was missing to interpret the observations.

The standard model of cosmology, called the Λ CDM model, is based on the assumption that DM is a classical pressureless gas ($P = 0$) and that DE is due to the cosmological constant Λ . DM could be made of (still hypothetical) particles called weakly interacting massive particles (WIMPs). These particles could be supersymmetric (SUSY) particles [9] with a mass in the GeV–TeV range. However, no evidence of such particles has been found at this day. In addition, although the Λ CDM model works extremely well at large (cosmological) scales, and can explain measurements of the cosmic microwave background (CMB) [1], it faces several difficulties at small (galactic) scales. Indeed, numerical simulations of CDM [10] predict that DM halos should be cuspy (with a central density diverging as r^{-1} when $r \rightarrow 0$) while observations [11] rather favor core density profiles. This is the so-called core–cusp problem [12]. On the other hand, since the Jeans length of classical matter at zero temperature vanishes, the Λ CDM model predicts that structures can form at all scales. This implies in particular an over-abundance of subhalos around the Milky Way. This leads to the missing satellite problem [13] and to the too big to fail problem [14]. The Λ CDM model therefore faces an important small-scale crisis [15].

There have been several attempts to solve the problems of the CDM model. For example, one can invoke the feedback of baryons to transform cusps into cores [16]. Alternatively, if DM is self-interacting [17], the “collisions” between particles can create an isothermal core instead of a cusp. Similarly, warm dark matter [18] explains the cores in terms of a balance between the gravitational attraction and the velocity dispersion of the particles. Another interesting suggestion is to take into account quantum mechanics or wave effects. Indeed, a general feature of quantum mechanics is to generate an effective pressure even at zero absolute temperature. This quantum pressure could prevent gravitational collapse. Interestingly, quantum effects are negligible at large scales, returning the classical Λ CDM model (and maintaining its virtues), but they manifest themselves at small scales and may solve the CDM crisis.

Some authors have considered the possibility that the DM particle is a fermion like a massive neutrino (see the Introduction of Ref. [19] for a short review and an exhaustive list of references). In that case, the gravitational attraction is balanced by the quantum pressure accounting for the Pauli exclusion principle like in white dwarf stars [20]. This leads to the formation of a fermion ball at $T = 0$. This quantum object is equivalent to a polytrope of index $n = 3/2$. Assuming that the smallest (ultra-compact) DM halo observed in the universe with a typical mass $M \sim 10^8 M_\odot$ and a typical radius $R \sim 1$ kpc corresponds to the ground state ($T = 0$) of the self-gravitating Fermi gas, one finds that the mass of the fermionic DM particle is $m = 170 \text{ eV}/c^2$ (see Appendix D of [21] and Section II. of [22]). Larger halos are described by the Fermi–Dirac distribution function at nonzero temperature. They have a core–halo structure made of a completely degenerate quantum core (fermion ball) surrounded by a classical isothermal halo (see, e.g., [23–25]). The fermion ball solves the core–cusp problem and the isothermal halo accounts for the flat rotation curves of the galaxies at large distances. The core mass–halo mass relation of fermionic DM halos has been determined in [22] from thermodynamical arguments, i.e., by maximizing the entropy at fixed mass and energy.

Other authors have considered the possibility that the DM particle is a boson, like an ultralight axion (ULA) (see the Introduction of Ref. [26] for a short review and an exhaustive list of references). At $T = 0$, the bosons are in the form of self-gravitating Bose–Einstein condensates (BECs). They are described by a single wavefunction which is determined by the Schrödinger–Poisson equations if the bosons are noninteracting or by the Gross–Pitaevskii–Poisson (GPP) equations if the bosons are self-interacting (see, e.g., [27,28]). This leads to the BECDM model that will be the main focus of the present paper. In this model, the gravitational attraction is balanced by the pressure (or the quantum potential) accounting for the Heisenberg uncertainty principle like in boson stars [29,30]. This leads to the formation of a quantum core often referred to as a soliton. If the bosons are self-interacting, there is an additional pressure arising from their scattering. If the interaction is repulsive the pressure is positive and counteracts the gravitational attraction. In the TF approximation, a self-gravitating BEC is equivalent to a polytrope of index $n = 1$. If the interaction is attractive (which is the case of the axion)

the pressure is negative and adds up to the gravitational attraction. In that case, BECDM halos can exist only below a maximum mass $M_{\max} = 1.012 \hbar / \sqrt{Gm|a_s|}$ first identified in [28].² Assuming that the smallest (ultra-compact) DM halo observed in the universe with a typical mass $M \sim 10^8 M_{\odot}$ and a typical radius $R \sim 1$ kpc corresponds to the ground state ($T = 0$) of the self-gravitating BEC, one finds that the mass of the bosonic DM particle is $m \sim 2.92 \times 10^{-22} \text{ eV}/c^2$ if it is noninteracting. These ultralight particles are not excluded by particle physics. Bosons with an attractive self-interaction sensibly have the same mass otherwise the minimum halo would be unstable ($M > M_{\max}$). Bosons with a repulsive self-interaction can have a mass up to 18 orders of magnitude larger than the mass of noninteracting bosons (see Appendix D of [21] and Section II. of [22] for more details). Larger DM halos have a core–halo structure made of a quantum core (soliton) surrounded by a halo of scalar radiation resulting from quantum interferences and presenting granularities. This core–halo structure is observed in direct numerical simulations of BECDM [34–41]. The density profile of the halo is consistent with the Navarro–Frenk–White (NFW) [10] profile of CDM simulations and with the observational Burkert [11] profile, both decreasing as r^{-3} at large distances, or with an isothermal profile characterized by an effective temperature T_{eff} decreasing as r^{-2} at large distances. The soliton solves the core–cusp problem and the approximately isothermal halo accounts for the flat rotation curves of the galaxies at large distances. The core mass–halo mass relation of bosonic DM halos was first determined numerically in [35] for noninteracting bosons and explained by heuristic arguments. It has also been determined from thermodynamical arguments in [22] for noninteracting and self-interacting bosons.

The formation of DM halos is a two-stages process. The first stage corresponds to the Jeans instability. An infinite homogeneous self-gravitating gas is dynamically unstable and forms clumps which are regions of over-density. This corresponds to the linear regime of structure formation. When the density of these clumps has grown significantly, the system enters in the nonlinear regime of structure formation. In that case, the gas undergoes gravitational collapse. It experiences free fall followed by a series of damped oscillations (due to an exchange between kinetic and potential energy) until it reaches a virialized state with a core–halo structure. This correspond to a process of collisionless violent relaxation [42] and gravitational cooling [43] (in the case of bosons). This fast collisionless relaxation, which takes place on a few dynamical times, is more relevant than the slow collisional relaxation which takes place on a timescale larger than the age of the universe (see, e.g., [25,44,45] for a detailed discussion).

The dynamical instability of an infinite homogeneous classical self-gravitating gas was first studied by Jeans [46] in a seminal paper. He identified a critical length $\lambda_J = 2\pi c_s / \sqrt{4\pi G\rho}$, where $c_s = \sqrt{P'(\rho)}$ is the speed of sound in the gas, above which the gas becomes unstable and fragments. The perturbations with a wavelength $\lambda > \lambda_J$ grow exponentially rapidly with time, while the perturbations with $\lambda < \lambda_J$ oscillate without attenuation as gravity-modified sound waves. Therefore, structure formation is suppressed on scales smaller than the Jeans length, and allowed on larger scales.³ The Jeans instability of classical barotropic gases and collisionless stellar systems is reviewed in [47]. This instability is fundamentally responsible for the formation of the large-scale structures observed in the Universe.

More recently, the Jeans stability analysis has been generalized for quantum particles in the context of the BECDM model. This study was initiated by Khlopov et al. [48] and Bianchi et al. [49] for a general relativistic SF described by the Klein–Gordon–Einstein (KGE) equations, and followed by Hu et al. [50] and Sikivie and Yang [51] for nonrelativistic BECs without self-interaction described by the Schrödinger–Poisson equations, by Chavanis [28] for nonrelativistic self-interacting BECs described

² This maximum mass has a nonrelativistic origin. It is physically different from the maximum mass of fermion stars [31] and boson stars [29,30,32,33] that is due to general relativity.

³ We note that the Jeans length vanishes in the pressureless CDM model ($c_s = 0 \Rightarrow \lambda_J = 0$). As a result, there is no “ground state” in this model so that structures can form at all scales. This leads to the different aspects of the CDM small-scale crisis mentioned above.

by the GPP equations, and by Suárez and Chavanis [52] for general relativistic self-interacting BECs described by the Gross–Pitaevskii–Einstein (GPE) equations. These authors showed that the formation of structures is suppressed at small scales even at $T = 0$ (unlike in the CDM model) because of the quantum pressure (Heisenberg) or the self-interaction of the bosons (in the repulsive case). They also determined the quantum Jeans length λ_J and the quantum Jeans mass M_J which provide an estimate of the minimum size and mass of BECDM halos (ground state).⁴ We refer to Suárez and Chavanis [52] for an exhaustive study of the Jeans instability in the BECDM model in Newtonian gravity and general relativity and for different estimates of the Jeans length and Jeans mass depending on the type of DM particle considered (noninteracting bosons, or bosons with a repulsive or an attractive self-interaction). The Jeans instability of rotating BECs in Newtonian gravity has been considered recently by Harko [53].

The original Jeans stability analysis [46] assumes that the universe is static (it was performed long before the discovery of the expansion of the universe). The study of structure formation in an expanding universe was first considered by Lifshitz [54] in general relativity and by Bonnor [55] (for a gas) and Gilbert [56] (for a stellar system) in Newtonian gravity. In that case, it is found that the perturbations above the Jeans length grow algebraically rapidly instead of exponentially rapidly as in the original Jeans analysis. The study of structure formation in the BECDM model in an expanding background was first studied by Bianchi et al. [49] for a general relativistic SF and by Sikivie and Yang [51] for nonrelativistic BECs without self-interaction. The case of self-interacting BECs was studied by Chavanis [57] and Suárez and Chavanis [58] in Newtonian gravity, and by Suárez and Matos [59] and Suárez and Chavanis [58] in general relativity.⁵

Recently, we have introduced a generalized GP equation—coupled to the Poisson equation—involving an arbitrary form of self-interaction (repulsive or attractive), an effective temperature, and a source of dissipation equivalent to a friction or a damping [61]. This new wave equation may have different interpretations: (i) It may describe dissipative self-gravitating BECs; (ii) it may provide a heuristic parametrization (on a coarse-grained scale) of the processes of violent relaxation and gravitational cooling experienced by a self-gravitating BEC fundamentally described by the ordinary GPP equations; (iii) it may provide a numerical algorithm to construct stable steady states of the ordinary GPP equations; (iv) it may arise from the fractal structure of space–time that manifests itself at very large (astrophysical) scales [62] in the theory of scale relativity [63]. In Ref. [61] we have initiated the study of the Jeans stability problem in the framework of these generalized GPP equations. We have established the general dispersion relation including dissipation effects and showed that the Jeans length is not affected by dissipation, thereby returning the expression of the quantum Jeans length for a self-interacting BEC obtained in our former work [28]. In the present paper, we study this dispersion relation in greater detail. We give particular consideration to the case of an attractive self-interaction (appropriate to the axion) which can induce an “hydrodynamical” (tachyonic) instability in addition to the gravitational instability. We determine the maximum growth rate of this instability with or without self-gravity and study how it depends on the scattering length of the bosons (through the squared speed of sound) and on the friction coefficient. We recover in particular limits the results previously obtained in the literature.

The paper is organized as follows. In Section 2, we recall the general equations of the problem and discuss their physical interpretations. We consider spatially inhomogeneous equilibrium states of the generalized GPP equations representing BECDM halos and derive the fundamental equation of quantum hydrostatic equilibrium. We also consider an infinite homogeneous self-gravitating

⁴ This is just an order of magnitude because the Jeans stability analysis is only valid in the linear regime of structure formation (it describes the initiation of the large-scale structures of the universe) while DM halos form in the nonlinear regime after a complicated process of free fall, violent relaxation, and gravitational cooling.

⁵ These studies are valid for a complex SF in Newtonian gravity and general relativity. They rely on the Madelung-de Broglie hydrodynamical representation of the GPP and KGE wave equations (see, e.g., [60] for details). Cosmological perturbations and gravitational instability in the case of a real SF in general relativity described by the KGE equations has been studied by numerous authors (see an exhaustive list of references in [52]).

BEC in a static or in an expanding universe and derive the linearized equations that can be used to study the formation of structures in the linear regime. In the following sections, we focus on an infinite homogeneous self-gravitating BEC in a static background and study the generalized Jeans dispersion relation. In Sections 3 and 4 we review previously obtained results in the frictionless limit and in the strong friction limit. In Section 5 we consider dissipative BECs with a repulsive or a vanishing self-interaction. In Section 6 we consider dissipative BECs with an attractive self-interaction. In Section 7 and in the conclusion we provide a summary of our results and a discussion. The Appendices bring additional results or present alternative manners to derive the basic equations of the problem.

2. Dissipative Self-Gravitating Bose–Einstein Condensates

2.1. Generalized Gross–Pitaevskii–Poisson Equations

We assume that DM is made of bosons (e.g., the axion) in the form of BECs. We use a nonrelativistic approach based on Newtonian gravity. In the standard BECDM model, the evolution of the wave function $\psi(\mathbf{r}, t)$ of the BEC is governed by the GPP equations (see, e.g., [27,28])

$$i\hbar \frac{\partial \psi}{\partial t} = -\frac{\hbar^2}{2m} \Delta \psi + m\Phi \psi + \frac{4\pi a_s \hbar^2}{m^2} |\psi|^2 \psi, \tag{1}$$

$$\Delta \Phi = 4\pi G |\psi|^2, \tag{2}$$

where $\Phi(\mathbf{r}, t)$ is the gravitational potential, m is the mass of the bosons, and a_s is their scattering length. The interaction between the bosons is repulsive when $a_s > 0$ and attractive when $a_s < 0$ (the bosons are noninteracting when $a_s = 0$). The mass density of the BEC is $\rho(\mathbf{r}, t) = |\psi|^2$.

To cover a greater variety of situations, we replace the GP Equation (1) by the generalized GP equation introduced in [61]

$$i\hbar \frac{\partial \psi}{\partial t} = -\frac{\hbar^2}{2m} \Delta \psi + \frac{4\pi a_s \hbar^2}{m^2} |\psi|^2 \psi + m\Phi \psi + m\Phi_{\text{ext}} \psi + 2k_B T \ln |\psi| \psi - i\frac{\hbar}{2} \zeta \left[\ln \left(\frac{\psi}{\psi^*} \right) - \left\langle \ln \left(\frac{\psi}{\psi^*} \right) \right\rangle \right] \psi \tag{3}$$

or, even more generally,

$$i\hbar \frac{\partial \psi}{\partial t} = -\frac{\hbar^2}{2m} \Delta \psi + m \frac{dV_{\text{int}}}{d|\psi|^2} \psi + m\Phi \psi + m\Phi_{\text{ext}} \psi + 2k_B T \ln |\psi| \psi - i\frac{\hbar}{2} \zeta \left[\ln \left(\frac{\psi}{\psi^*} \right) - \left\langle \ln \left(\frac{\psi}{\psi^*} \right) \right\rangle \right] \psi. \tag{4}$$

The first term is the kinetic term which accounts for the Heisenberg uncertainty principle. The second term takes into account the self-interaction of the bosons. The third term accounts for the self-gravity of the BEC. The fourth term is an external potential which takes into account the possible presence of a central black hole, the influence of dark energy (cosmological constant), tidal effects etc. The fifth term is an effective temperature term and the sixth term is a friction (or damping) term.⁶ The usual GP Equation (1) is recovered when $T = \zeta = 0$, $V_{\text{int}} = (2\pi a_s \hbar^2 / m^3) |\psi|^4$, and $\Phi_{\text{ext}} = 0$. It is convenient to introduce the total potential

$$V(|\psi|^2) = V_{\text{int}}(|\psi|^2) + V_{\text{th}}(|\psi|^2) \quad \text{with} \quad V_{\text{th}}(|\psi|^2) = \frac{k_B T}{m} |\psi|^2 (\ln |\psi|^2 - 1), \tag{5}$$

⁶ The interpretation of these terms will become clear in the hydrodynamical representation of the generalized GPP equations given in the following section. In a sense, we can obtain the wave Equation (4) from the quantum damped Euler Equations (14)–(19) by using the “inverse” Madelung transformation. However, this wave equation may have a more profound meaning as explained in interpretation (ii) below.

where V_{int} takes into account self-interaction effects and V_{th} takes into account thermal effects. We can then rewrite Equation (4) as

$$i\hbar \frac{\partial \psi}{\partial t} = -\frac{\hbar^2}{2m} \Delta \psi + m \frac{dV}{d|\psi|^2} \psi + m\Phi \psi + m\Phi_{\text{ext}} \psi - i\frac{\hbar}{2} \xi \left[\ln \left(\frac{\psi}{\psi^*} \right) - \left\langle \ln \left(\frac{\psi}{\psi^*} \right) \right\rangle \right] \psi. \tag{6}$$

In the following we take $\Phi_{\text{ext}} = 0$ since it will play no role in our analysis.

Finally, we take into account the expansion of the universe. In an expanding background,⁷ the generalized GPP equations take the form (see Refs. [57,58,60,64] and Appendix C)

$$i\hbar \frac{\partial \psi}{\partial t} + \frac{3}{2} i\hbar H \psi = -\frac{\hbar^2}{2ma^2} \Delta \psi + m \frac{dV}{d|\psi|^2} \psi + m\Phi \psi - i\frac{\hbar}{2} \xi \left[\ln \left(\frac{\psi}{\psi^*} \right) - \left\langle \ln \left(\frac{\psi}{\psi^*} \right) \right\rangle \right] \psi, \tag{7}$$

$$\frac{\Delta \Phi}{4\pi G a^2} = |\psi|^2 - \frac{3H^2}{8\pi G}, \tag{8}$$

where $a(t)$ is the scale factor and $H = \dot{a}/a$ is the Hubble parameter. Multiplying Equation (7) par ψ^* and subtracting the resulting equation with its complex conjugate, we obtain after simplification

$$\frac{\partial}{\partial t} (a^3 |\psi|^2) + \nabla \cdot \left[\frac{i\hbar a}{2m} (\psi \nabla \psi^* - \psi^* \nabla \psi) \right] = 0. \tag{9}$$

This equation has the form of a continuity equation

$$\frac{\partial}{\partial t} (\rho a^3) + \nabla \cdot \mathbf{J} = 0 \tag{10}$$

with the current

$$\mathbf{J} = \frac{i\hbar a}{2m} (\psi \nabla \psi^* - \psi^* \nabla \psi). \tag{11}$$

These equations express the conservation of mass $M = \int \rho a^3 d\mathbf{r}$ in an expanding background.

We can give different interpretations to the generalized GPP Equations (7) and (8) introduced in [61]:

(i) When applied to the problem of structure formation in a cosmological context, the generalized GPP equations can describe a dissipative self-gravitating BEC with an arbitrary potential of self-interaction $V(|\psi|^2)$. Dissipative effects may be important in the early universe and the effective temperature T may account for thermal fluctuations.

(ii) When applied to a single DM halo (with $a = 1$), we have argued in [61] that the generalized GPP equations can provide a simple parametrization (on a coarse-grained scale) of the original GPP Equations (1) and (2) taking into account the processes of violent relaxation and gravitational cooling. In that case, T is an effective temperature like in the Lynden–Bell [42] theory of violent relaxation and ξ is a damping coefficient which is related to a form of nonlinear Landau damping experienced by a collisionless self-gravitating system.⁸ The generalized GPP equations relax towards a stable equilibrium state with a core–halo structure. The quantum core (soliton) corresponds to the ground state solution of the GPP Equations (1) and (2). It stems from the equilibrium between the gravitational force and the quantum pressure force arising from the Heisenberg uncertainty principle or from the self-interaction of the bosons (when $a_s > 0$). These quantum terms are important at “small” scales (≤ 1 kpc). They stabilize the system against gravitational collapse and solve the cusp–core problem. The halo results from the quantum interferences of excited states. It stems from the equilibrium between

⁷ We assume that the background is not affected by the damping.

⁸ In a forthcoming paper [65] we will provide a heuristic derivation of the generalized GPP Equations (7) and (8) by using a procedure similar to the one developed in Ref. [66] in connection to the Lynden–Bell theory of violent relaxation [42].

the gravitational force and the pressure force due to the effective temperature. The temperature term is important at “large” scales ($\gg 1$ kpc). It accounts for the flat rotation curves of the galaxies which have a constant circular velocity (e.g., $v_\infty = (2k_B T/m)^{1/2} \sim 153$ km/s for the medium spiral).⁹

(iii) When applied to a single DM halo (with $a = 1$), we have shown in [61] that the generalized GPP equations relax towards an equilibrium state which minimizes the energy at fixed mass. As a result, the generalized GPP equations provide a useful numerical algorithm to construct stable steady states of the ordinary GPP Equations (1) and (2), which are minima of energy at fixed mass. This is interesting because it is generally difficult to solve the nonlinear eigenvalue problem determining a steady state of the ordinary GPP equations and make sure that the solution is dynamically stable. The stationary solution reached by the generalized GPP equations is guaranteed to be a stable steady state of the ordinary GPP equations (see Appendix B of [26] and [65]).

(iv) In a speculative paper [62], inspired by Nottale’s theory of scale relativity [63], we have suggested that space–time may become fractal at very large (astrophysical) scales. In that case, the trajectories of the particles are nondifferentiable and the deterministic equations must be replaced by stochastic ones (in the sense of Nottale). This leads to a form of Schrödinger equation with a diffusion-like coefficient \mathcal{D} (called the fractal fluctuation parameter) playing the role of $\hbar^2/2m$ in the usual Schrödinger equation of quantum mechanics. In that case, “quantum” effects are a manifestation of the fractal structure of space–time at the cosmic scale. Similarly, the effective temperature T (fluctuation) and the friction ζ (dissipation) may be intrinsic properties of space–time. The dissipation may be due to the interaction of the system with an external environment (e.g., a Dirac-like aether) and the temperature may represent the temperature of the vacuum if it has fluctuations. In our approach [62] the temperature and the friction arise from a single formalism. They correspond to the real and imaginary parts of the complex friction coefficient present in the scale covariant equation of dynamics and they satisfy a form of fluctuation-dissipation theorem (see Appendix B).

2.2. Madelung Transformation

Writing the wave function as

$$\psi(\mathbf{r}, t) = \sqrt{\rho(\mathbf{r}, t)} e^{iS(\mathbf{r}, t)/\hbar}, \tag{12}$$

where $\rho(\mathbf{r}, t)$ is the mass density and $S(\mathbf{r}, t) = (\hbar/2i) \ln(\psi/\psi^*)$ is the action, and making the Madelung [68] transformation

$$\rho(\mathbf{r}, t) = |\psi|^2 \quad \text{and} \quad \mathbf{u} = \frac{\nabla S}{ma} = \frac{i\hbar}{2ma} \frac{\psi \nabla \psi^* - \psi^* \nabla \psi}{|\psi|^2}, \tag{13}$$

⁹ If we take $m \sim 2.92 \times 10^{-22}$ eV/c² for the boson mass, we obtain a temperature $T \sim 4.41 \times 10^{-25}$ K. Such a small temperature is clearly unphysical, confirming that T is an *effective* temperature [61]. In addition, the condensation temperature of bosons is $T_c = 2\pi\hbar^2 \rho^{2/3} / (m^{5/3} k_B \zeta(3/2)^{2/3}) \sim 4.82 \times 10^{36}$ K for $\rho \sim 7.02 \times 10^{-3} M_\odot/\text{pc}^3$ (medium spiral) so that $T \ll T_c$. This shows that the isothermal halo is an out-of-equilibrium structure (otherwise it would have condensed). It is important to note that the effective temperature T in the generalized GPP Equations (7) and (8) is completely different from the thermodynamical temperature T_{thermo} in the Zaremba–Nikuni–Griffin (ZNG) approach to the BECs [67]. The ZNG equations describe the collisional relaxation of a gas of bosons and the interactions between the condensate and the cloud of uncondensed bosons. By contrast, we are considering a collisionless (mean field) regime, equivalent to $T_{\text{thermo}} = 0$, where we are far from thermal equilibrium. For self-gravitating bosons, the processes of gravitational cooling and violent collisionless relaxation arising from the strong fluctuations of the gravitational potential during free fall lead to a quantum core (soliton) + a halo of scalar radiation with an effective temperature T . Therefore, the generalized GPP Equations (7) and (8) are physically different from the ZNG equations and have a completely different domain of validity (collisionless versus collisional).

where $\mathbf{u}(\mathbf{r}, t)$ is the velocity field, it is shown in [61] (see also [57,58,60,64] and Appendix C in an expanding background) that the generalized GPP Equations (7) and (8) can be written under the form of hydrodynamic equations as

$$\frac{\partial \rho}{\partial t} + 3H\rho + \frac{1}{a} \nabla \cdot (\rho \mathbf{u}) = 0, \tag{14}$$

$$\frac{\partial S}{\partial t} + \frac{(\nabla S)^2}{2ma^2} = -Q - m\Phi - mV'(\rho) - \zeta(S - \langle S \rangle), \tag{15}$$

$$\frac{\partial \mathbf{u}}{\partial t} + H\mathbf{u} + \frac{1}{a}(\mathbf{u} \cdot \nabla)\mathbf{u} = -\frac{1}{\rho a} \nabla P - \frac{1}{a} \nabla \Phi - \frac{1}{ma} \nabla Q - \zeta \mathbf{u}, \tag{16}$$

$$\frac{\Delta \Phi}{4\pi G a^2} = \rho - \frac{3H^2}{8\pi G}, \tag{17}$$

where

$$Q = -\frac{\hbar^2}{2ma^2} \frac{\Delta \sqrt{\rho}}{\sqrt{\rho}} = -\frac{\hbar^2}{4ma^2} \left[\frac{\Delta \rho}{\rho} - \frac{1}{2} \frac{(\nabla \rho)^2}{\rho^2} \right] \tag{18}$$

is the quantum potential taking into account the Heisenberg uncertainty principle. The pressure is a function $P = P(\rho)$ of the density (the gas is barotropic) which is determined by the potential $V(\rho)$ through the relation (see Appendix A)

$$P(\rho) = \rho V'(\rho) - V(\rho) = \rho^2 \left[\frac{V(\rho)}{\rho} \right]' \quad \Rightarrow \quad P'(\rho) = \rho V''(\rho). \tag{19}$$

The squared speed of sound is

$$c_s^2 = P'(\rho) = \rho V''(\rho). \tag{20}$$

In terms of the density, the relation (5) can be written as

$$V(\rho) = V_{\text{int}}(\rho) + V_{\text{th}}(\rho) \quad \text{with} \quad V_{\text{th}}(\rho) = \frac{k_B T}{m} \rho (\ln \rho - 1), \tag{21}$$

yielding

$$P(\rho) = P_{\text{int}}(\rho) + P_{\text{th}}(\rho) \quad \text{with} \quad P_{\text{th}}(\rho) = \rho \frac{k_B T}{m}. \tag{22}$$

For the standard BEC, we have

$$V_{\text{int}}(\rho) = \frac{2\pi a_s \hbar^2}{m^3} \rho^2 \quad \text{and} \quad P_{\text{int}} = \frac{2\pi a_s \hbar^2}{m^3} \rho^2. \tag{23}$$

The total speed of sound is given by

$$c_s^2 = \frac{4\pi a_s \hbar^2}{m^3} \rho + \frac{k_B T}{m}. \tag{24}$$

We note that the logarithmic potential $V_{\text{th}}(\rho)$ taking into account (effective) thermal effects is associated with an isothermal equation of state. On the other hand, the power-law potential $V_{\text{int}}(\rho)$ taking into account the self-interaction of the bosons is associated with a polytropic equation of state of index $\gamma = 2$.

The hydrodynamic Equations (14)–(17) are called the quantum damped Euler–Poisson equations. Equation (14) is the equation of continuity. It is equivalent to Equation (10) with $\mathbf{J} = a^2 \rho \mathbf{u}$. Equation (15) is the quantum damped Hamilton–Jacobi (or Bernoulli) equation. Equation (16), obtained by taking the gradient of Equation (15), is the quantum damped Euler equation. Equation (17) is the Poisson equation. We clearly see on these equations that T has the interpretation of a temperature and that ζ has

the interpretation of a friction coefficient. When $\hbar = 0$,¹⁰ we get the classical damped Euler–Poisson equations [66]. When $\xi = 0$, we get the quantum Euler–Poisson equations associated with the usual GPP equations [28]. When $\xi = \hbar = 0$ we get the classical Euler–Poisson equations [8]. In the strong friction limit $\xi \rightarrow +\infty$, we can neglect the advection term in the momentum Equation (16) and we get the quantum Smoluchowski–Poisson (SP) equations [69]:

$$\frac{\partial \rho}{\partial t} + 3H\rho = \frac{1}{\xi a^2} \nabla \cdot \left(\nabla P + \rho \nabla \Phi + \frac{\rho}{m} \nabla Q \right), \tag{25}$$

$$\frac{\Delta \Phi}{4\pi G a^2} = \rho - \frac{3H^2}{8\pi G}. \tag{26}$$

When $\xi \rightarrow +\infty$ and $\hbar = 0$, we get the classical Smoluchowski–Poisson equations [70]. It is interesting to note that at a formal level, the damped GPP Equations (7) and (8) allow us to make a connection between the Schrödinger equation of quantum mechanics ($\xi = 0$) and the Smoluchowski equation of Brownian theory ($\xi \rightarrow +\infty$) [61].

By using the Madelung transformation, the generalized GPP Equations (7) and (8) have been written in the form of hydrodynamic equations involving a quantum potential taking into account the Heisenberg uncertainty principle, a pressure force arising from the self-interaction of the bosons (or from effective thermal effects), and a friction force. This transformation allows us to treat the BEC as a quantum fluid (superfluid) and to apply standard methods developed in astrophysics as discussed below.

Remark 1. *In this paper, we have taken into account dissipative effects in the BEC by using a generalized wave equation [Equation (7)] leading, through the Madelung transformation, to a damped quantum Euler equation [Equation (16)] involving a linear friction force $-\xi \mathbf{u}$. One could also consider a generalized wave equation associated (via the Madelung transformation) to a quantum Navier–Stokes equation involving a viscous term $\nu \Delta \mathbf{u}$. This type of generalized wave equations has been considered in Section 7 and in Appendix L of [71], and in Appendix L of [61].*

2.3. Spatially Inhomogeneous Equilibrium States: DM Halos

We first apply the generalized GPP Equations (7) and (8), or equivalently the quantum damped Euler–Poisson Equations (14)–(17), to DM halos. We take $a = 1$ since the expansion of the universe is negligible at the scale of DM halos.

2.3.1. Core–Halo Structure

It is shown in [61] that the generalized GPP equations satisfy an H -theorem for a generalized free energy F and generically relax towards a stable equilibrium state which minimizes F at fixed mass M .¹¹ The condition of quantum hydrostatic equilibrium, which corresponds to the steady state of the quantum Euler Equation (16), writes

$$\frac{\rho}{m} \nabla Q + \nabla P + \rho \nabla \Phi = \mathbf{0}. \tag{27}$$

¹⁰ Here and in the following, $\hbar = 0$ described either classical particles or BECs in the Thomas–Fermi (TF) limit where the quantum potential can be neglected.

¹¹ The H -theorem and the relaxation towards an equilibrium state are due to the friction term $\xi > 0$ which provides a source of dissipation and implies the irreversibility of the generalized GPP Equations (7) and (8). By contrast, the ordinary GPP Equations (1) and (2) are reversible. Their relaxation towards a quasisteady state is due to gravitational cooling and can be understood only at a coarse-grained level. It is in this sense that the generalized GPP Equations (7) and (8) provide a parametrization of the GPP Equations (1) and (2) taking into account the processes of gravitational cooling and violent relaxation (see the interpretation (ii) of these equations given in Section 2.1).

Combined with the Poisson Equation (17), we obtain the fundamental differential equation of quantum hydrostatic equilibrium

$$\frac{\hbar^2}{2m^2} \Delta \left(\frac{\Delta \sqrt{\rho}}{\sqrt{\rho}} \right) - \nabla \cdot \left(\frac{\nabla P}{\rho} \right) = 4\pi G\rho. \tag{28}$$

If we decompose the pressure according to Equation (22), and if we consider the case of a standard BEC (23) to be explicit, the foregoing equations become

$$\frac{\rho}{m} \nabla Q + \nabla P_{\text{int}} + \nabla P_{\text{th}} + \rho \nabla \Phi = \mathbf{0} \tag{29}$$

and

$$\frac{\hbar^2}{2m^2} \Delta \left(\frac{\Delta \sqrt{\rho}}{\sqrt{\rho}} \right) - \frac{4\pi a_s \hbar^2}{m^3} \Delta \rho - \frac{k_B T}{m} \Delta \ln \rho = 4\pi G\rho. \tag{30}$$

They describe the balance between the quantum potential taking into account the Heisenberg uncertainty principle, the pressure due to the self-interaction of the bosons, the pressure due to effective thermal effects, and the self-gravity. The solutions of these equations have a “core–halo” structure with a quantum core (soliton) and an isothermal halo (see [45] for explicit calculations in the TF limit). These solutions are consistent with the structure of large DM halos that are obtained in direct numerical simulations of BECDM [34–41].

Remark 2. A stationary solution of the generalized GPP Equations (7) and (8) with $a = 1$ is of the form $\psi(\mathbf{r}, t) = \phi(\mathbf{r})e^{-iEt/\hbar}$, where the real quantities $\phi(\mathbf{r}) = \sqrt{\rho(\mathbf{r})}$ and E (eigenenergy) are determined by the eigenvalue problem

$$-\frac{\hbar^2}{2m} \Delta \phi + m [\Phi + V'(\rho)] \phi = E\phi, \tag{31}$$

$$\Delta \Phi = 4\pi G\phi^2. \tag{32}$$

Dividing Equation (31) by ϕ , we get

$$Q + m\Phi + mV'(\rho) = E. \tag{33}$$

Taking the gradient of this equation and using Equation (19), we recover the condition of quantum hydrostatic equilibrium, Equation (27). The foregoing equations can also be obtained by extremizing the free energy at fixed mass [61]. This variational principle shows that the eigenenergy is equal to the total chemical potential ($E = \mu_{\text{tot}}$).

2.3.2. Quantum Core (Soliton)

In the core, we can neglect thermal effects and take $P_{\text{th}} = 0$. In that case, we obtain

$$\frac{\rho}{m} \nabla Q + \nabla P_{\text{int}} + \rho \nabla \Phi = \mathbf{0} \tag{34}$$

and

$$\frac{\hbar^2}{2m^2} \Delta \left(\frac{\Delta \sqrt{\rho}}{\sqrt{\rho}} \right) - \frac{4\pi a_s \hbar^2}{m^3} \Delta \rho = 4\pi G\rho. \tag{35}$$

The equilibrium of the core results from the balance between the quantum potential, the self-interaction of the bosons, and the gravitational attraction. Equation (35) has been solved analytically (using a Gaussian ansatz) in [28] and numerically in [72], for an arbitrary (repulsive or attractive) self-interaction. It describes a compact quantum core (soliton). Because of quantum effects, the central density is finite instead of diverging as in the CDM model. Therefore, quantum mechanics can solve the cusp–core problem.

2.3.3. Isothermal Halo

In the halo, we can neglect quantum effects and take $Q = 0$ and $P_{\text{int}} = 0$. In that case, we obtain

$$\nabla P_{\text{th}} + \rho \nabla \Phi = \mathbf{0} \tag{36}$$

and

$$-\frac{k_B T}{m} \Delta \ln \rho = 4\pi G \rho. \tag{37}$$

The equilibrium of the halo is due to the balance between the thermal pressure and the gravitational attraction. Equation (37) is equivalent to the Boltzmann–Poisson equation or to the Emden equation [20]. This equation has no simple analytical solution and must be solved numerically. However, its asymptotic behavior is known analytically [20]. The density of a self-gravitating isothermal halo decreases as $\rho(r) \sim k_B T / (2\pi G m r^2)$ for $r \rightarrow +\infty$, corresponding to an accumulated mass $M(r) \sim 2k_B T r / G m$ increasing linearly with r . This leads to flat rotation curves

$$v^2(r) = \frac{GM(r)}{r} \rightarrow v_\infty^2 = \frac{2k_B T}{m} \tag{38}$$

in agreement with the observations [8].

2.3.4. Conclusions

In conclusion, the physical meaning of the generalized GPP Equations (7) and (8) is clear. The friction allows the system to relax towards a stable equilibrium state with a “core–halo” structure. The quantum core can solve the core–cusp problem and the isothermal halo accounts for the flat rotation curves of the galaxies. This core–halo structure is in agreement with the phenomenology of BECDM halos.

2.4. Infinite Homogeneous Distribution: Generalized Jeans Problem

We now apply the generalized GPP Equations (7) and (8), or equivalently the quantum damped Euler–Poisson Equations (14)–(17), to the universe as a whole. We first study the formation of structures in a static universe ($a = 1$). Specifically, we study the linear dynamical stability of an infinite homogeneous self-gravitating BEC with density ρ and velocity $\mathbf{u} = \mathbf{0}$ described by the quantum damped Euler–Poisson Equations (14)–(17). This is a generalization of the classical Jeans problem [46] to a dissipative quantum fluid.¹²

¹² As is well-known, the Jeans approach suffers from a mathematical inconsistency at the start. Indeed, an infinite homogeneous self-gravitating system cannot be in static equilibrium since there are no pressure gradients to balance the gravitational force. In other words, we cannot simultaneously satisfy the condition of hydrostatic equilibrium $\nabla P + \rho \nabla \Phi = \mathbf{0}$, which reduces to $\nabla \Phi = \mathbf{0}$ for a barotropic fluid with a constant density ρ , and the Poisson equation $\Delta \Phi = 4\pi G \rho$ [8]. Jeans [46] removed this inconsistency by assuming that the Poisson equation describes only the relationship between the perturbed gravitational potential and the perturbed density. However, this assumption seems to be ad hoc and is known as the *Jeans swindle* [8]. In fact, the detailed discussion of the Jeans “swindle” provided by Kiessling [73] and Joyce et al. [74,75] has demonstrated that there is no swindle in the Jeans analysis. These authors have shown that the gravitational force created by an infinite and uniform distribution of particles in a static universe is well-defined provided that it is summed symmetrically about

Considering a small perturbation about the equilibrium state and linearizing the hydrodynamic Equations (14)–(17), we obtain

$$\frac{\partial \delta}{\partial t} + \nabla \cdot \mathbf{u} = 0, \tag{39}$$

$$\frac{\partial \mathbf{u}}{\partial t} = -c_s^2 \nabla \delta - \nabla \delta \Phi + \frac{\hbar^2}{4m^2} \nabla (\Delta \delta) - \zeta \mathbf{u}, \tag{40}$$

$$\Delta \delta \Phi = 4\pi G \rho \delta, \tag{41}$$

where $c_s^2 = P'(\rho)$ is the squared speed of sound and $\delta(\mathbf{r}, t) = \delta\rho(\mathbf{r}, t)/\rho$ is the density contrast. Taking the time derivative of Equation (39) and the divergence of Equation (40), and using the Poisson Equation (41), we obtain a single equation for the density contrast

$$\frac{\partial^2 \delta}{\partial t^2} + \zeta \frac{\partial \delta}{\partial t} = -\frac{\hbar^2}{4m^2} \Delta^2 \delta + c_s^2 \Delta \delta + 4\pi G \rho \delta. \tag{42}$$

Expanding the solutions of this equation into plane waves of the form $\delta(\mathbf{r}, t) \propto \exp[i(\mathbf{k} \cdot \mathbf{r} - \omega t)]$, we obtain the dispersion relation (see Appendix M of [61])

$$\omega^2 + i\zeta\omega = \frac{\hbar^2 k^4}{4m^2} + c_s^2 k^2 - 4\pi G \rho. \tag{43}$$

The Jeans wavenumber k_J , corresponding to $\omega = 0$, is determined by the quadratic equation

$$\frac{\hbar^2 k_J^4}{4m^2} + c_s^2 k_J^2 - 4\pi G \rho = 0. \tag{44}$$

It is given by

$$k_J^2 = \frac{2m^2}{\hbar^2} \left(-c_s^2 + \sqrt{c_s^4 + \frac{4\pi G \rho \hbar^2}{m^2}} \right). \tag{45}$$

This general expression of the quantum Jeans wavenumber, valid for possibly self-interacting bosons, was first given in [28]. As noted in [61], the Jeans wavenumber is not altered by dissipative effects (the friction parameter ζ does not appear in its expression). The general dispersion relation (43) is studied in detail in Sections 3–6 below. We shall review and connect different limits have already been investigated in the literature.

2.5. Structure Formation in an Expanding Universe: Generalized Bonnor Equation

Finally, we consider the formation of structures in the framework of the generalized GPP Equations (7) and (8), or equivalently in the framework of the quantum damped Euler–Poisson Equations (14)–(17), in an expanding universe. Specifically, we study the linear dynamical stability of an infinite homogeneous self-gravitating BEC with density $\rho_b(t)$ and velocity $\mathbf{u} = \mathbf{0}$ (in the comoving frame) described by the quantum damped Euler–Poisson Equations (14)–(17). This is a generalization of the classical Bonnor problem [55] to a dissipative quantum fluid. In that case, an infinite homogeneous

each particle. This leads to a *modified* Poisson equation of the form $\Delta \Phi = 4\pi G(\rho - \bar{\rho})$ where $\bar{\rho}$ is the average density. In that case, a uniform distribution $\rho = \bar{\rho}$ is an exact solution of the equations of the problem. Modifying the Poisson in this way (or by introducing a screening length κ^{-1} in the interaction and letting $\kappa \rightarrow 0$) is not a “swindle” but rather a well-defined and rigorous mathematical procedure [73] to treat the problem (see [47,52,76] for additional discussion).

distribution of matter is an equilibrium solution of the hydrodynamic equations and this problem is mathematically well-posed without swindle or without the need to modify the Poisson equation.¹³

For the homogeneous solution $\rho(\mathbf{r}, t) = \rho_b(t)$, $S(\mathbf{r}, t) = S_0(t)$, $\mathbf{u}(\mathbf{r}, t) = \mathbf{0}$ and $\Phi(\mathbf{r}, t) = 0$, corresponding to a wavefunction

$$\psi_b(t) = \sqrt{\rho_b(t)} e^{iS_0(t)/\hbar}, \tag{46}$$

the hydrodynamic Equations (14)–(17) reduce to

$$\frac{d\rho_b}{dt} + 3H\rho_b = 0, \tag{47}$$

$$\frac{dS_0}{dt} = -mV'(\rho_b), \tag{48}$$

$$H^2 = \frac{8\pi G\rho_b}{3}. \tag{49}$$

Equations (47) and (49) are the same equations as in the CDM model. They correspond to the Friedmann [78,79] equations for a nonrelativistic (or pressureless) cosmic fluid. Therefore, quantum mechanics does not affect the evolution of the background in the nonrelativistic regime. Equation (47) is readily integrated into

$$\rho_b \propto a^{-3}, \tag{50}$$

expressing the conservation of mass. Then, Equation (49) determines the evolution of the scale factor. This leads to the Einstein–de Sitter (EdS) [80] solution

$$a \propto t^{2/3}, \quad H = \frac{2}{3t}, \quad \rho_b = \frac{1}{6\pi Gt^2}. \tag{51}$$

For a standard BEC, Equation (48) can be readily integrated with the aid of Equations (23) and (51) yielding $S_0 = 2a_s\hbar^2 / (3Gm^2t)$.

We now consider a perturbation about the homogeneous background and write

$$\rho = \rho_b(t)[1 + \delta(\mathbf{r}, t)], \tag{52}$$

where $\delta(\mathbf{r}, t) = \delta\rho(\mathbf{r}, t) / \rho_b(t)$ is the density contrast. The wavefunction can be written as

$$\psi = \sqrt{\rho_b(1 + \delta)} e^{iS/\hbar}. \tag{53}$$

We stress that at this stage, we do not assume that δ is small. We can then rewrite the hydrodynamic Equations (14)–(17) in terms of the density contrast as

$$\frac{\partial\delta}{\partial t} + \frac{1}{a}\nabla \cdot [(1 + \delta)\mathbf{u}] = 0, \tag{54}$$

$$\frac{\partial S}{\partial t} + \frac{(\nabla S)^2}{2ma^2} = \frac{\hbar^2}{2ma^2} \frac{\Delta\sqrt{1 + \delta}}{\sqrt{1 + \delta}} - m\Phi - mV'[\rho_b(1 + \delta)] - \zeta(S - \langle S \rangle), \tag{55}$$

¹³ In cosmology, when we work in the comoving frame, the expansion of the universe introduces a sort of “neutralizing background” with a negative density $-3H^2/8\pi G$ in the Poisson Equation (17), like in the Jellium model of plasma physics. In that case, an infinite homogeneous self-gravitating medium can be in static equilibrium in the comoving frame [77]. Therefore, the Jeans instability mechanism is relevant to understand the formation of DM halos and galaxies in the homogeneous early universe.

$$\frac{\partial \mathbf{u}}{\partial t} + H\mathbf{u} + \frac{1}{a}(\mathbf{u} \cdot \nabla)\mathbf{u} = -\frac{c_s^2}{(1+\delta)a}\nabla\delta - \frac{1}{a}\nabla\Phi + \frac{\hbar^2}{2m^2a^3}\nabla\left(\frac{\Delta\sqrt{1+\delta}}{\sqrt{1+\delta}}\right) - \zeta\mathbf{u}, \tag{56}$$

$$\Delta\Phi = 4\pi G\rho_b a^2\delta. \tag{57}$$

In the strong friction limit $\zeta \rightarrow +\infty$, they reduce to

$$\frac{\partial\delta}{\partial t} = \frac{1}{\zeta a^2}\nabla \cdot \left[c_s^2\nabla\delta + (1+\delta)\nabla\Phi - \frac{\hbar^2}{2m^2a^2}(1+\delta)\nabla\left(\frac{\Delta\sqrt{1+\delta}}{\sqrt{1+\delta}}\right) \right]. \tag{58}$$

If we now consider a small perturbation $\delta \ll 1$, we can linearize the foregoing equations. The wavefunction (53) can be written as $\psi = \psi_b + \delta\psi$ with

$$\delta\psi = \psi_b \left(\frac{\delta}{2} + i\frac{\delta S}{\hbar} \right), \tag{59}$$

where we have defined $\delta S = S - S_0 \ll 1$. We also have $\rho = |\psi|^2 = (\psi_b + \delta\psi)(\psi_b^* + \delta\psi^*) \simeq |\psi_b|^2 + \psi_b\delta\psi^* + \psi_b^*\delta\psi$ so that $\delta\rho = \psi_b\delta\psi^* + \psi_b^*\delta\psi$. On the other hand, the linearized hydrodynamic Equations (54)–(57) are

$$\frac{\partial\delta}{\partial t} + \frac{1}{a}\nabla \cdot \mathbf{u} = 0, \tag{60}$$

$$\frac{\partial\delta S}{\partial t} = \frac{\hbar^2}{4ma^2}\Delta\delta - m\Phi - mc_s^2\delta - \zeta(\delta S - \langle\delta S\rangle), \tag{61}$$

$$\frac{\partial\mathbf{u}}{\partial t} + H\mathbf{u} = -\frac{1}{a}c_s^2\nabla\delta - \frac{1}{a}\nabla\delta\Phi + \frac{\hbar^2}{4m^2a^3}\nabla(\Delta\delta) - \zeta\mathbf{u}, \tag{62}$$

$$\Delta\Phi = 4\pi G\rho_b a^2\delta. \tag{63}$$

They can be combined into a single equation for the density contrast

$$\frac{\partial^2\delta}{\partial t^2} + (2H + \zeta)\frac{\partial\delta}{\partial t} = \frac{c_s^2}{a^2}\Delta\delta + 4\pi G\rho_b\delta - \frac{\hbar^2}{4m^2a^4}\Delta^2\delta. \tag{64}$$

In the strong friction limit $\zeta \rightarrow +\infty$, Equation (64) becomes

$$\zeta\frac{\partial\delta}{\partial t} = \frac{c_s^2}{a^2}\Delta\delta + 4\pi G\rho_b\delta - \frac{\hbar^2}{4m^2a^4}\Delta^2\delta. \tag{65}$$

If we decompose the perturbations into normal modes of the form $\delta(\mathbf{r}, t) = \delta_{\mathbf{k}}(t)e^{i\mathbf{k}\cdot\mathbf{r}}$ etc., we obtain

$$\mathbf{u} = \frac{i\mathbf{k}}{ma}\delta S, \quad \delta S = \frac{ma^2}{k^2}\frac{\partial\delta}{\partial t}, \quad \mathbf{u} = -\frac{a}{i}\frac{\mathbf{k}}{k^2}\frac{\partial\delta}{\partial t}, \tag{66}$$

$$\Phi = -\frac{4\pi G\rho_b a^2\delta}{k^2}, \quad \frac{\delta\psi}{\psi_b} = \frac{\delta}{2} + \frac{ima^2}{\hbar k^2}\frac{\partial\delta}{\partial t}, \tag{67}$$

where $\delta(t)$ is determined by the equation

$$\ddot{\delta} + (2H + \zeta)\dot{\delta} + \left(\frac{\hbar^2 k^4}{4m^2 a^4} + \frac{c_s^2 k^2}{a^2} - 4\pi G\rho_b \right) \delta = 0. \tag{68}$$

For brevity, we have not written the dependance of $\delta_{\mathbf{k}}(t)$ on the wavenumber \mathbf{k} . In the strong friction limit $\zeta \rightarrow +\infty$, Equation (68) becomes

$$\zeta\dot{\delta} + \left(\frac{\hbar^2 k^4}{4m^2 a^4} + \frac{c_s^2 k^2}{a^2} - 4\pi G\rho_b \right) \delta = 0. \tag{69}$$

In a static universe ($a = 1$), writing $\delta(t) \propto e^{-i\omega t}$, we recover the dispersion relation (43) [61]. In order to study Equation (68), it is more convenient to express the density contrast in terms of a rather than in terms of t . Making the change of variables from Equation (51) valid in the EdS universe, we find that Equation (68) is replaced by

$$\frac{d^2\delta}{da^2} + \frac{3}{2a}(1 + \chi a^{3/2})\frac{d\delta}{da} + \frac{3}{2a^2} \left(\frac{\hbar^2 k^4}{16\pi G\rho_b m^2 a^4} + \frac{c_s^2 k^2}{4\pi G\rho_b a^2} - 1 \right) \delta = 0, \tag{70}$$

where we have defined the constant χ through the relation $\chi = \zeta t/a^{3/2}$ (recall that $t/a^{3/2}$ is constant according to Equation (51)). In the strong friction limit $\zeta \rightarrow +\infty$, Equation (70) becomes

$$\chi \frac{d\delta}{da} + \frac{1}{a^{5/2}} \left(\frac{\hbar^2 k^4}{16\pi G\rho_b m^2 a^4} + \frac{c_s^2 k^2}{4\pi G\rho_b a^2} - 1 \right) \delta = 0. \tag{71}$$

These equations will be studied in a specific paper [65]. When $\zeta = \hbar = 0$, we recover the results of Bonnor [55] for classical particles. When $\zeta = 0$ and $c_s = 0$, we recover the results of Bianchi et al. [49] and Sikivie and Yang [51] for noninteracting bosons. When $\zeta = 0$, we recover the results of Suárez and Matos [59] and Chavanis [57] for possibly interacting bosons.¹⁴ Analytical solutions of Equation (70) when $\zeta = 0$ are given in [57] and illustrated in [58]. It is shown that the typical Jeans length is the same in a static and in an expanding universe. However, the evolution of the perturbation is different. In the stable regime ($k > k_J(a)$) the perturbation is oscillating in the two cases but in the unstable regime ($k < k_J(a)$) the growth of the perturbation is algebraic in an expanding universe and exponential in a static universe.

For a dissipative cold classical gas ($\hbar = c_s^2 = 0$), or for noninteracting bosons in the TF limit, Equation (70) reduces to

$$\frac{d^2\delta}{da^2} + \frac{3}{2a}(1 + \chi a^{3/2})\frac{d\delta}{da} - \frac{3}{2a^2}\delta = 0. \tag{72}$$

In the dissipationless limit $\zeta \rightarrow 0$, Equation (72) becomes

$$\frac{d^2\delta}{da^2} + \frac{3}{2a}\frac{d\delta}{da} - \frac{3}{2a^2}\delta = 0. \tag{73}$$

Its independent solutions are [77]

$$\delta_+ \propto a, \quad \delta_- \propto a^{-3/2}. \tag{74}$$

The first solution describes a growing mode and the second solution describes a decaying mode. In the strong friction limit $\zeta \rightarrow +\infty$, Equation (72) becomes

$$\chi \frac{d\delta}{da} - \frac{1}{a^{5/2}}\delta = 0. \tag{75}$$

Its solution is

$$\delta = \delta_{\max} e^{-\frac{2}{3\chi a^{3/2}}}. \tag{76}$$

The density contrast starts from $\delta = 0$ at $a = 0$, increases, and tends to a constant δ_{\max} for $a \rightarrow +\infty$. This extreme case ($\zeta \gg 1$) illustrates the effect of the friction which is to saturate the growth

¹⁴ The results of Refs. [57,59] were obtained independently. Suárez and Matos [59] started from the KGE equations and took at the end the nonrelativistic limit $c \rightarrow +\infty$. Chavanis [57] directly started from the GPP equations valid in the nonrelativistic limit. The generalization of Equation (70) in general relativity was obtained by Suárez and Chavanis [58].

of the density contrast even in the linear regime. For a finite value of ξ , the independent solutions of Equation (72) are

$$\delta_+ \propto \frac{5}{3}\chi^{2/3}ae^{-\chi a^{3/2}} + \left(\frac{10}{9\chi a^{3/2}} - \frac{5}{3}\right) \left[\Gamma\left(\frac{5}{3}, \chi a^{3/2}\right) - \Gamma\left(\frac{5}{3}\right)\right], \tag{77}$$

and

$$\delta_- \propto \frac{1}{\chi a^{3/2}} - \frac{3}{2}, \tag{78}$$

where $\Gamma(z)$ is the Gamma function and $\Gamma(a, z)$ is the incomplete Gamma function. The growing solution behaves as $\chi^{2/3}a$ for $a \rightarrow 0$ (like δ_+ in Equation (74)) and tends to a finite value $\Gamma(8/3) = 1.50458\dots$ for $a \rightarrow +\infty$ (like δ in Equation (76)). The decaying solution behaves as $1/(\chi a^{3/2})$ for $a \rightarrow 0$ (like δ_- in Equation (74)) and vanishes at a finite time corresponding to $a_* = (2/3\chi)^{2/3}$. These solutions are plotted in Figure 1.

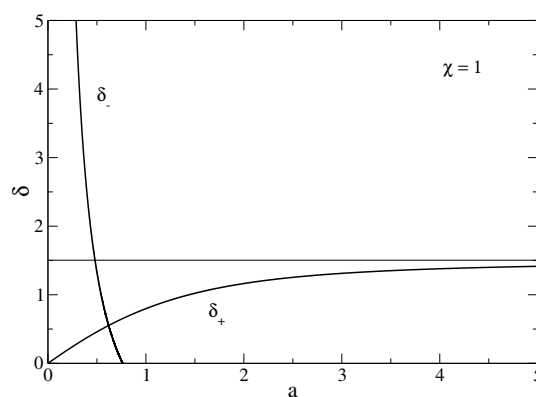


Figure 1. Growing and decaying modes of a dissipative noninteracting BEC in the TF limit ($\hbar = c_s^2 = 0$) in an expanding background. We have taken $\chi = 1$ for illustration.

2.6. Fermionic DM

Although the previous formalism has been developed for self-gravitating bosons in the form of BECs, it can also be applied to self-gravitating fermions. In that case, we must take into account the Pauli exclusion principle that prevents two fermions to occupy the same quantum state. In a semiclassical approach, the Pauli exclusion principle creates a pressure P_{Pauli} which plays a role similar to the pressure P_{int} arising from the self-interaction of the bosons. Therefore, we just have to replace P_{int} by P_{Pauli} in the previous formalism.

In the nonrelativistic limit, the equation of state of the Fermi gas at $T = 0$ is

$$P(\rho) = \frac{1}{20} \left(\frac{3}{\pi}\right)^{2/3} \frac{\hbar^2}{m^{8/3}} \rho^{5/3}. \tag{79}$$

Using the results of Section 2.2 and Appendix A, the enthalpy and the potential are given by

$$h(\rho) = \frac{1}{8} \left(\frac{3}{\pi}\right)^{2/3} \frac{\hbar^2}{m^{8/3}} \rho^{2/3}, \quad V(\rho) = \frac{3}{40} \left(\frac{3}{\pi}\right)^{2/3} \frac{\hbar^2}{m^{8/3}} \rho^{5/3}. \tag{80}$$

This leads to a generalized wave equation of the form

$$i\hbar \frac{\partial \psi}{\partial t} = -\frac{\hbar^2}{2m} \Delta \psi + \frac{1}{8} \left(\frac{3}{\pi}\right)^{2/3} \frac{\hbar^2}{m^{5/3}} |\psi|^{4/3} \psi + m\Phi\psi + m\Phi_{\text{ext}}\psi + 2k_B T \ln |\psi| - i\frac{\hbar}{2} \xi \left[\ln\left(\frac{\psi}{\psi^*}\right) - \left\langle \ln\left(\frac{\psi}{\psi^*}\right) \right\rangle \right] \psi. \tag{81}$$

On the other hand, the squared speed of sound that is needed in the Jeans analysis is

$$c_s^2 = \frac{1}{12} \left(\frac{3}{\pi} \right)^{2/3} \frac{h^2}{m^{8/3}} \rho^{2/3}. \tag{82}$$

We can take into account the expansion of the universe as in the previous sections.

In the ultrarelativistic limit, the equation of state of the Fermi gas at $T = 0$ is

$$P(\rho) = \frac{1}{8} \left(\frac{3}{\pi} \right)^{1/3} \frac{hc}{m^{4/3}} \rho^{4/3}. \tag{83}$$

Using the results of Section 2.2 and Appendix A, the enthalpy and the potential are given by

$$h(\rho) = \frac{1}{2} \left(\frac{3}{\pi} \right)^{1/3} \frac{hc}{m^{4/3}} \rho^{1/3}, \quad V(\rho) = \frac{3}{8} \left(\frac{3}{\pi} \right)^{1/3} \frac{hc}{m^{4/3}} \rho^{4/3}. \tag{84}$$

This leads to a generalized wave equation of the form

$$i\hbar \frac{\partial \psi}{\partial t} = -\frac{\hbar^2}{2m} \Delta \psi + \frac{1}{2} \left(\frac{3}{\pi} \right)^{1/3} \frac{hc}{m^{1/3}} |\psi|^{2/3} \psi + m\Phi\psi + m\Phi_{\text{ext}}\psi + 2k_B T \ln |\psi| \psi - i\frac{\hbar}{2} \zeta \left[\ln \left(\frac{\psi}{\psi^*} \right) - \left\langle \ln \left(\frac{\psi}{\psi^*} \right) \right\rangle \right] \psi. \tag{85}$$

The squared speed of sound that is needed in the Jeans analysis is

$$c_s^2 = \frac{1}{6} \left(\frac{3}{\pi} \right)^{1/3} \frac{hc}{m^{4/3}} \rho^{1/3}. \tag{86}$$

We can take into account the expansion of the universe as in the previous sections.

The wave Equations (81) and (85) with $\zeta = T = 0$ are expected to display a process of violent relaxation leading to a fermion ball at $T = 0$ surrounded by a halo of scalar radiation. This is similar to the process of gravitational cooling experienced by the GPP Equations (1) and (2) for bosons (the fermion ball is the counterpart of the bosonic condensate). The coarse-grained Equations (81) and (85), with the friction and temperature terms retained, parameterize the process of violent relaxation. Note that these equations also take into account the Heisenberg uncertainty principle. This provides an additional small-scale regularization, in addition to the Pauli exclusion principle.

3. The Dissipationless Case $\zeta = 0$

We first review the Jeans instability problem in the dissipationless case ($\zeta = 0$) treated in previous papers. In that case, the system is described by the quantum Euler-Poisson equations and the dispersion relation is given by [28]

$$\omega^2 = \frac{\hbar^2 k^4}{4m^2} + c_s^2 k^2 - 4\pi G\rho. \tag{87}$$

The squared pulsation is real. When $\omega^2 > 0$, the pulsation is real and the perturbation behaves with time as $e^{-i\omega t}$, i.e., it oscillates with a pulsation ω (with $\omega = \pm\sqrt{\omega^2}$). When $\omega^2 < 0$, the pulsation is imaginary ($\omega = i\gamma$) and the perturbation behaves with time as $e^{\gamma t}$, i.e., it evolves exponentially with time with a rate γ (with $\gamma = \pm\sqrt{-\omega^2}$). There is a growing mode ($\gamma_+ > 0$) and a decaying mode ($\gamma_- < 0$).

3.1. The Case $\hbar = G = 0$

In the classical (or TF) + nongravitational limit ($\hbar = G = 0$), the dispersion relation (87) reduces to

$$\omega^2 = c_s^2 k^2. \tag{88}$$

It is plotted in Figure 2.

When $c_s^2 > 0$, the squared pulsation is positive ($\omega^2 > 0$). The system is stable for all modes k . The perturbation oscillates with a pulsation $\omega = \pm c_s k$ corresponding to a sound wave (this is associated with the concept of phonons in the language of superfluidity [81]).

When $c_s = 0$, the squared pulsation vanishes ($\omega = 0$). The perturbation is stationary.

When $c_s^2 < 0$, the squared pulsation is negative ($\omega^2 < 0$). The system is unstable for all modes k . The perturbation evolves exponentially rapidly with a rate $\gamma = \pm (|c_s^2|)^{1/2} k$. The growth rate tends to $+\infty$ when $k \rightarrow +\infty$.

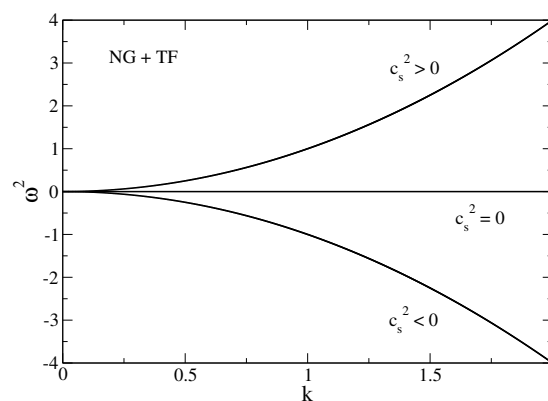


Figure 2. Dispersion relation for dissipationless BECs in the nongravitational + TF limit ($G = \hbar = 0$).

3.2. The Case $\hbar = 0$

The classical limit ($\hbar = 0$) has been treated by Jeans [46] in a seminal paper. His results also apply to self-gravitating BECs with a repulsive self-interaction in the TF limit. In that case, the dispersion relation (87) reduces to

$$\omega^2 = c_s^2 k^2 - 4\pi G\rho. \tag{89}$$

It is plotted in Figure 3.

When $c_s^2 > 0$, the classical (or TF) Jeans wavenumber is

$$k_J = \left(\frac{4\pi G\rho}{c_s^2} \right)^{1/2}. \tag{90}$$

It is due to the interplay between the attractive gravity and the repulsive pressure (or self-interaction). For $k = k_J$, the pulsation vanishes ($\omega = 0$) and the perturbation is stationary. For $k > k_J$, the squared pulsation is positive ($\omega^2 > 0$). The system is stable for these modes. The perturbation oscillates with a pulsation

$$\omega = \pm \sqrt{c_s^2 k^2 - 4\pi G\rho}. \tag{91}$$

This corresponds to a gravity-modified sound wave. For $k \rightarrow +\infty$, we have $\omega \sim \pm c_s k$. For $k < k_J$, the squared pulsation is negative ($\omega^2 < 0$). The system is unstable for these modes. The perturbation evolves exponentially rapidly with a rate

$$\gamma = \pm \sqrt{-c_s^2 k^2 + 4\pi G \rho}. \tag{92}$$

For $k = 0$, we have $\gamma = \pm \sqrt{4\pi G \rho}$. The growth rate is maximum at $k_m = 0$ (infinite wavelength) with value $\gamma_{\max} = \sqrt{4\pi G \rho}$.

When $c_s = 0$, the dispersion relation writes

$$\omega^2 = -4\pi G \rho. \tag{93}$$

The system is unstable for all modes ($k_j \rightarrow +\infty$). The perturbation evolves exponentially rapidly with a rate $\gamma = \pm \sqrt{4\pi G \rho}$.

When $c_s^2 < 0$, the squared pulsation is negative ($\omega^2 < 0$). The system is unstable for all modes. The perturbation evolves exponentially rapidly with a rate

$$\gamma = \pm \sqrt{|c_s^2| k^2 + 4\pi G \rho}. \tag{94}$$

For $k = 0$, we have $\gamma = \pm \sqrt{4\pi G \rho}$. For $k \rightarrow +\infty$, we have $\gamma \sim \pm (|c_s^2|)^{1/2} k$. The growth rate tends to $+\infty$ when $k \rightarrow +\infty$.

The noninteracting regime corresponds to $k \ll (4\pi G \rho / |c_s^2|)^{1/2}$ and the nongravitational regime corresponds to $k \gg (4\pi G \rho / |c_s^2|)^{1/2}$.

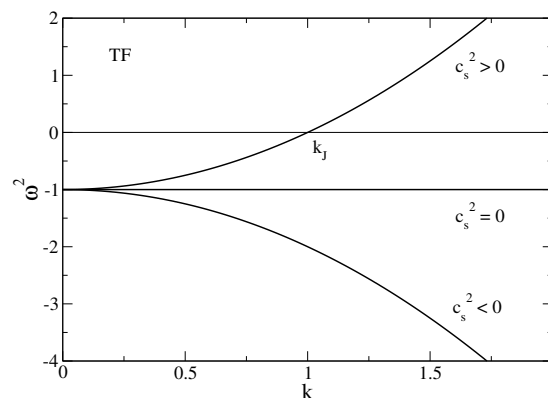


Figure 3. Dispersion relation for dissipationless self-gravitating BECs in the TF limit ($\hbar = 0$). We have normalized the wavenumber by $(4\pi G \rho / |c_s^2|)^{1/2}$ and the pulsation by $(4\pi G \rho)^{1/2}$. This is equivalent to taking $4\pi G = \rho = |c_s^2| = 1$ in the dimensional equations.

3.3. The Case $G = 0$

The nongravitational limit ($G = 0$) has been treated by Bogoliubov [82] in a seminal paper on superfluidity. In that case, the dispersion relation (87) reduces to

$$\omega^2 = \frac{\hbar^2 k^4}{4m^2} + c_s^2 k^2. \tag{95}$$

It is plotted in Figure 4. Bogoliubov [82] considered the case of bosons with a repulsive self-interaction (corresponding to $c_s^2 > 0$) and determined the excitation spectrum of the bosons at $T = 0$ —equivalent to the dispersion relation (95)—from a microscopic theory. At short wavelengths ($k \rightarrow +\infty$), or for noninteracting bosons, we recover the free-particle energy $\omega \sim \hbar k^2 / 2m$. At long wavelengths ($k \rightarrow 0$), the excitation spectrum reduces to the phonon solution $\omega \sim \pm c_s k$. The crossover

from the particle-like region to the collective phonon region occurs at a wavenumber $k_c \sim mc_s/\hbar$. This shows how the self-interaction changes the qualitative nature of low-energy excitations in a BEC. The linear spectrum at long wavelengths provides the key to superfluid behavior and was a triumph of Bogoliubov’s pioneering calculations. The derivation of the dispersion relation (95) from the GP equation, or from its hydrodynamic representation, and the consideration of bosons with an attractive self-interaction (corresponding to $c_s^2 < 0$), appeared later in the BEC literature [81]. In the hydrodynamic description, the linear spectrum is almost obvious. The dispersion relation (95) was also specifically considered by Khlopov et al. [48], Chavanis [28] and Guth et al. [83] as a particular case of their study of self-gravitating BECs. This limit may apply, for example, to axions in the early universe which have an attractive self-interaction and a negligible self-gravity. In the relativistic regime, this leads to the notion of axitons which were studied by Kolb and Tkachev [84].

When $c_s^2 > 0$, the squared pulsation is positive ($\omega^2 > 0$). The system is stable for all modes. The perturbation oscillates with a pulsation

$$\omega = \pm \sqrt{\frac{\hbar^2 k^4}{4m^2} + c_s^2 k^2}. \tag{96}$$

For $k \rightarrow 0$, we have $\omega \sim \pm c_s k$. For $k \rightarrow +\infty$, we have $\omega \sim \pm \hbar k^2 / 2m$.

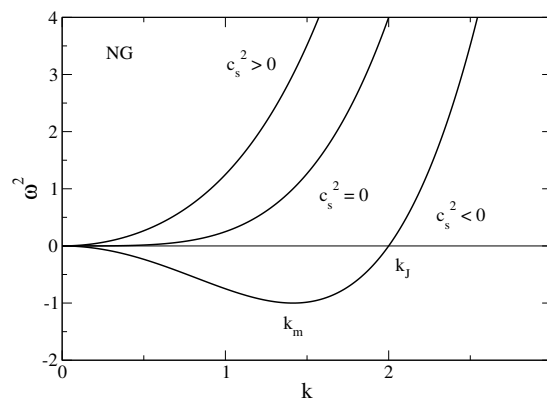


Figure 4. Dispersion relation for dissipationless BECs in the nongravitational limit ($G = 0$). We have normalized the wavenumber by $(m^2|c_s^2|/\hbar^2)^{1/2}$ and the pulsation by $m|c_s^2|/\hbar$. This is equivalent to taking $m = |c_s^2| = \hbar = 1$ in the dimensional equations.

When $c_s = 0$, the dispersion relation writes

$$\omega = \pm \frac{\hbar k^2}{2m}. \tag{97}$$

This is the dispersion relation associated with a free particle whose kinetic energy is $E = p^2/2m$ when we use the Einstein–de Broglie relations $E = \hbar\omega$ and $\mathbf{p} = \hbar\mathbf{k}$.

When $c_s^2 < 0$, we can define an effective Jeans wavenumber¹⁵

$$k_J = \left(\frac{4m^2|c_s^2|}{\hbar^2} \right)^{1/2}. \tag{98}$$

¹⁵ We call this critical wavenumber a “Jeans wavenumber” by an abuse of language since there is no gravity in the present situation. The instability is a purely “hydrodynamical” (tachyonic) instability. This terminology will make sense in the general case (see Section 3.4) where the instability is due to the combined effect of self-gravity and self-interaction.

It is due to the interplay between the attractive self-interaction and the repulsive quantum potential. For $k = k_J$, the pulsation vanishes ($\omega = 0$) and the perturbation is stationary. For $k > k_J$, the squared pulsation is positive ($\omega^2 > 0$). The system is stable for these modes. The perturbation oscillates with a pulsation

$$\omega = \pm \sqrt{\frac{\hbar^2 k^4}{4m^2} - |c_s^2| k^2}. \tag{99}$$

For $k \rightarrow +\infty$, we have $\omega \sim \pm \hbar k^2 / 2m$. For $k < k_J$, the squared pulsation is negative ($\omega^2 < 0$). The system is unstable for these modes. The perturbation evolves exponentially rapidly with a rate

$$\gamma = \pm \sqrt{-\frac{\hbar^2 k^4}{4m^2} + |c_s^2| k^2}. \tag{100}$$

For $k \rightarrow 0$, we have $\gamma \sim \pm (|c_s^2|)^{1/2} k$. The growth rate is maximum at the wavenumber

$$k_m = \left(\frac{2m^2 |c_s^2|}{\hbar^2} \right)^{1/2} \tag{101}$$

with value

$$\gamma_{\max} = \frac{m |c_s^2|}{\hbar}. \tag{102}$$

We note that $k_J = \sqrt{2} k_m$.

The noninteracting regime corresponds to $k \gg m |c_s^2|^{1/2} / \hbar$ and the TF regime corresponds to $k \ll m |c_s^2|^{1/2} / \hbar$.

3.4. The General Case

The dispersion relation (87) has been studied in the general case by Khlopov et al. [48] and Chavanis [28].¹⁶ It is plotted in Figure 5. The generalized Jeans wavenumber k_J is given by [28]

$$k_J^2 = \frac{2m^2}{\hbar^2} \left[\sqrt{c_s^4 + \frac{4\pi G \rho \hbar^2}{m^2}} - c_s^2 \right]. \tag{103}$$

It is due to the interplay between the attractive gravity, the repulsive quantum potential and the (attractive or repulsive) self-interaction. A repulsive self-interaction increases the quantum Jeans length while an attractive self-interaction decreases the quantum Jeans length (see Figure 6). For $k = k_J$, the pulsation vanishes ($\omega = 0$) and the perturbation is stationary. For $k > k_J$, the squared pulsation is positive ($\omega^2 > 0$). The system is stable for these modes. For $k < k_J$, the squared pulsation is negative ($\omega^2 < 0$). The system is unstable for these modes.

¹⁶ Khlopov et al. [48] developed a general relativistic approach based on the KGE equations while Chavanis [28] developed a nonrelativistic approach based on the GPP equations. The nonrelativistic approach of Chavanis [28] was extended to general relativity by Suárez and Chavanis [52]. Their treatment goes beyond some limitations of the approach of Khlopov et al. [48] as explained in footnote 7 of [52].

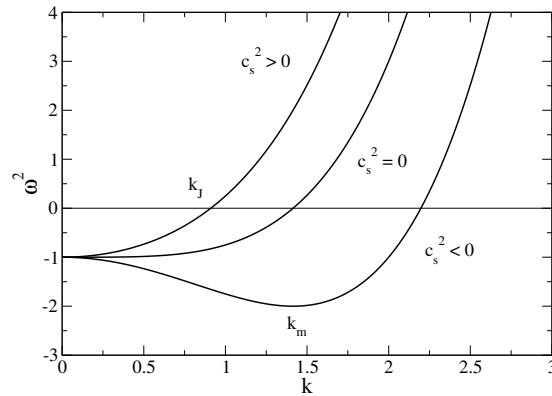


Figure 5. Dispersion relation for dissipationless self-gravitating BECs in the general case. We have normalized the wavenumber by $(4\pi G\rho m^2/\hbar^2)^{1/4}$, the pulsation by $(4\pi G\rho)^{1/2}$ and the squared speed of sound by $(4\pi G\rho\hbar^2/m^2)^{1/2}$. This is equivalent to taking $4\pi G = \rho = m = \hbar = 1$ in the dimensional equations. We have selected $c_s^2 = 1, 0, -1$.

We first assume that $c_s^2 > 0$. For $k > k_J$, the perturbation oscillates with a pulsation

$$\omega = \pm \sqrt{\frac{\hbar^2 k^4}{4m^2} + c_s^2 k^2 - 4\pi G\rho}. \tag{104}$$

For $k \rightarrow +\infty$, we have $\omega \sim \pm \hbar k^2/2m$. For $k < k_J$, the perturbation evolves exponentially rapidly with a rate

$$\gamma = \pm \sqrt{-\frac{\hbar^2 k^4}{4m^2} - c_s^2 k^2 + 4\pi G\rho}. \tag{105}$$

For $k = 0$, we have $\gamma = \pm \sqrt{4\pi G\rho}$. The growth rate is maximum at $k_m = 0$ (infinite wavelength) with value $\gamma_{\max} = \sqrt{4\pi G\rho}$.

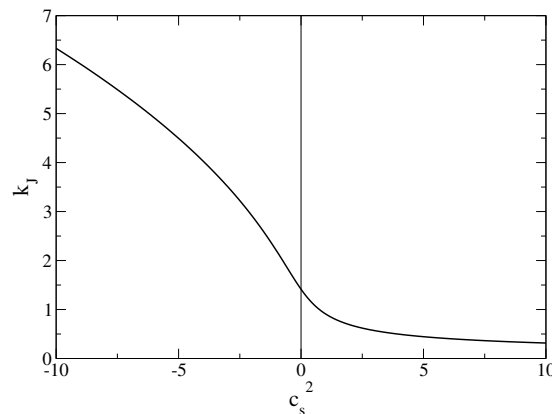


Figure 6. Jeans wavenumber of self-gravitating BECs as a function of the the squared speed of sound. We have normalized the Jeans wavenumber by $(4\pi G\rho m^2/\hbar^2)^{1/4}$ and the squared speed of sound by $(4\pi G\rho\hbar^2/m^2)^{1/2}$. This is equivalent to taking $4\pi G = \rho = m = \hbar = 1$ in the dimensional equations. For $c_s = 0$, we have $k_J = (16\pi G\rho m^2/\hbar^2)^{1/4}$. For $c_s^2 \rightarrow +\infty$, we have $k_J \sim (4\pi G\rho/c_s^2)^{1/2}$. For $c_s^2 \rightarrow -\infty$, we have $k_J \sim (4m^2|c_s^2|/\hbar^2)^{1/2}$.

The special case $c_s^2 = 0$, corresponding to noninteracting bosons, has been studied specifically by Khlopov et al. [48], Bianchi et al. [49], Hu et al. [50], Sikivie and Yang [51], and Chavanis [28]. In that case, the dispersion relation (87) writes

$$\omega^2 = \frac{\hbar^2 k^4}{4m^2} - 4\pi G\rho. \tag{106}$$

This is the gravitational analogue of the Bogoliubov [82] energy spectrum of the excitation of a weakly interacting BEC (Appendix D). For large wavenumbers (small wavelengths), the quasi-particle energy tends to the kinetic energy of an individual gas particle and $\omega \sim \hbar k^2/2m$. The quantum Jeans wavenumber of noninteracting bosons is

$$k_J = \left(\frac{16\pi G\rho m^2}{\hbar^2} \right)^{1/4}. \tag{107}$$

It is due to the interplay between the attractive gravity and the repulsive quantum potential. We finally assume that $c_s^2 < 0$. For $k > k_J$, the perturbation oscillates with a pulsation

$$\omega = \pm \sqrt{\frac{\hbar^2 k^4}{4m^2} - |c_s^2| k^2 - 4\pi G\rho}. \tag{108}$$

For $k \rightarrow +\infty$ we have $\omega \sim \pm \hbar k^2/2m$. For $k < k_J$, the perturbation evolves exponentially rapidly with a rate

$$\gamma = \pm \sqrt{-\frac{\hbar^2 k^4}{4m^2} + |c_s^2| k^2 + 4\pi G\rho}. \tag{109}$$

For $k = 0$, we have $\gamma = \pm \sqrt{4\pi G\rho}$. The growth rate is maximum at

$$k_m = \left(\frac{2m^2 |c_s^2|}{\hbar^2} \right)^{1/2} \tag{110}$$

with value

$$\gamma_{\max} = \sqrt{\frac{m^2 c_s^4}{\hbar^2} + 4\pi G\rho}. \tag{111}$$

Since $\gamma_{\max} > \sqrt{4\pi G\rho}$, an attractive self-interaction increases the growth rate of the Jeans instability.

4. The Strong Friction Limit $\zeta \rightarrow +\infty$

We now consider the Jeans instability problem in the overdamped limit ($\zeta \rightarrow +\infty$). This limit has been studied by Chavanis [69]. In that case, the system is described by the quantum Smoluchowski-Poisson equations and the dispersion relation is given by [69]

$$i\zeta\omega = \frac{\hbar^2 k^4}{4m^2} + c_s^2 k^2 - 4\pi G\rho. \tag{112}$$

The pulsation ω is imaginary. Introducing the growth ($\gamma > 0$) or damping ($\gamma < 0$) rate $\gamma = -i\omega$, the dispersion relation (112) can be rewritten as

$$\gamma = -\frac{1}{\zeta} \left(\frac{\hbar^2 k^4}{4m^2} + c_s^2 k^2 - 4\pi G\rho \right). \tag{113}$$

The perturbation behaves with time as $e^{\gamma t}$, i.e., it evolves exponentially with a rate γ .

4.1. The Case $\hbar = G = 0$

In the classical (or TF) + nongravitational limit ($\hbar = G = 0$), the dispersion relation (113) reduces to

$$\gamma = -\frac{1}{\xi} c_s^2 k^2. \tag{114}$$

It is plotted in Figure 7.

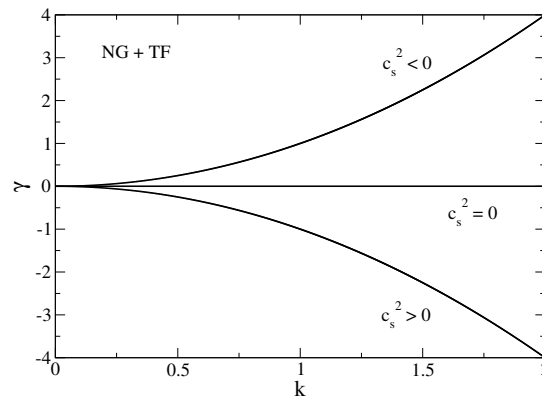


Figure 7. Exponential rate for overdamped BECs in the nongravitational + TF limit ($G = \hbar = 0$).

When $c_s^2 > 0$, the perturbation decays exponentially rapidly ($\gamma < 0$). The system is stable for all modes k .

When $c_s = 0$, the perturbation is stationary ($\gamma = 0$).

When $c_s^2 < 0$, the perturbation grows exponentially rapidly ($\gamma > 0$). The system is unstable for all modes k . The growth rate tends to $+\infty$ when $k \rightarrow +\infty$.

4.2. The Case $\hbar = 0$

In the classical (or TF) limit ($\hbar = 0$), the dispersion relation (113) reduces to

$$\gamma = -\frac{1}{\xi} (c_s^2 k^2 - 4\pi G \rho). \tag{115}$$

It is plotted in Figure 8.

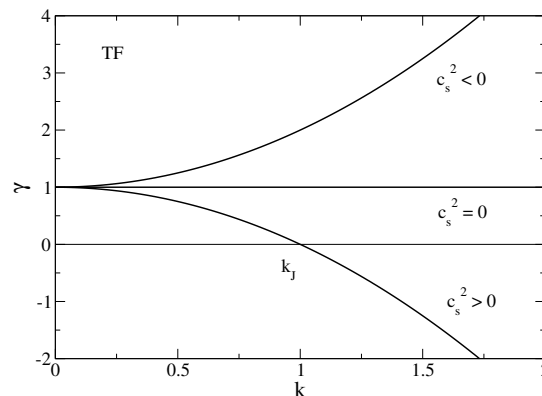


Figure 8. Exponential rate γ for overdamped self-gravitating BECs in the TF limit ($\hbar = 0$). We have normalized the wavenumber by $(4\pi G \rho / |c_s^2|)^{1/2}$ and the rate by $4\pi G \rho / \xi$. This is equivalent to taking $4\pi G = \rho = |c_s^2| = \xi = 1$ in the dimensional equations.

When $c_s^2 > 0$, the classical Jeans wavenumber is

$$k_J = \left(\frac{4\pi G\rho}{c_s^2} \right)^{1/2}. \tag{116}$$

It coincides with Equation (90). For $k = k_J$, the perturbation is stationary ($\gamma = 0$). For $k > k_J$, the perturbation decays exponentially rapidly ($\gamma < 0$). The system is stable for these modes. For $k \rightarrow +\infty$, we have $\gamma \sim -\frac{1}{\xi}c_s^2k^2$. For $k < k_J$, the perturbation grows exponentially rapidly ($\gamma > 0$). The system is unstable for these modes. For $k = 0$, we have $\gamma = 4\pi G\rho/\xi$. The growth rate is maximum at $k_m = 0$ (infinite wavelength) with value $\gamma_{\max} = 4\pi G\rho/\xi$.

When $c_s = 0$, the dispersion relation writes

$$\gamma = \frac{4\pi G\rho}{\xi}. \tag{117}$$

The perturbation grows exponentially rapidly ($\gamma > 0$). The system is unstable for all modes ($k_J \rightarrow +\infty$).

When $c_s^2 < 0$, the perturbation grows exponentially rapidly ($\gamma > 0$). The system is unstable for all modes. For $k = 0$, we have $\gamma = 4\pi G\rho/\xi$. For $k \rightarrow +\infty$, we have $\gamma \sim |c_s^2|k^2/\xi$. The growth rate tends to $+\infty$ when $k \rightarrow +\infty$.

4.3. The Case $G = 0$

In the nongravitational limit ($G = 0$), the dispersion relation (113) reduces to

$$\gamma = -\frac{1}{\xi} \left(\frac{\hbar^2 k^4}{4m^2} + c_s^2 k^2 \right). \tag{118}$$

It is plotted in Figure 9.

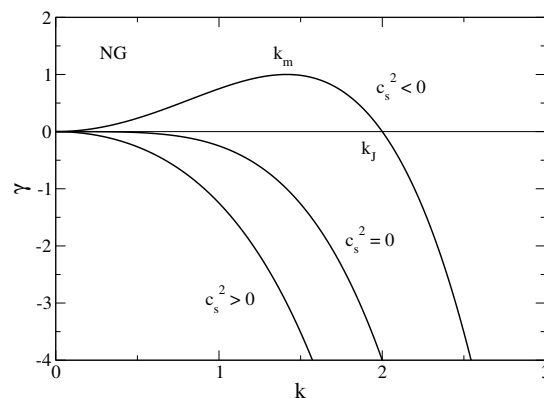


Figure 9. Exponential rate γ for overdamped BECs in the nongravitational limit ($G = 0$). We have normalized the wavenumber by $(m^2|c_s^2|/\hbar^2)^{1/2}$ and the rate by $m^2c_s^4/\hbar^2\xi$. This is equivalent to taking $m = |c_s^2| = \hbar = \xi = 1$ in the dimensional equations.

When $c_s^2 > 0$, the perturbation decays exponentially rapidly ($\gamma < 0$). The system is stable for all modes. For $k \rightarrow 0$, we have $\gamma \sim -\frac{1}{\xi}c_s^2k^2$. For $k \rightarrow +\infty$, we have $\gamma \sim -\hbar^2k^4/4\xi m^2$.

When $c_s^2 = 0$, the dispersion relation writes

$$\gamma = -\frac{\hbar^2 k^4}{4\xi m^2}. \tag{119}$$

The perturbation decays exponentially rapidly ($\gamma < 0$). The system is stable for all modes.

When $c_s^2 < 0$, we can define an effective Jeans wavenumber (see footnote 15)

$$k_J = \left(\frac{4m^2|c_s^2|}{\hbar^2} \right)^{1/2}. \tag{120}$$

It coincides with Equation (98). For $k = k_J$, the perturbation is stationary ($\gamma = 0$). For $k > k_J$, the perturbation decays exponentially rapidly ($\gamma < 0$). The system is stable for these modes. For $k \rightarrow +\infty$, we have $\gamma \sim -\hbar^2 k^4 / 4\zeta m^2$. For $k < k_J$, the perturbation grows exponentially rapidly ($\gamma > 0$). The system is unstable for these modes. For $k \rightarrow 0$, we have $\gamma \sim \frac{1}{\zeta} |c_s^2| k^2$. The growth rate is maximum at the wavenumber

$$k_m = \left(\frac{2m^2|c_s^2|}{\hbar^2} \right)^{1/2} \tag{121}$$

with value

$$\gamma_{\max} = \frac{m^2 c_s^4}{\zeta \hbar^2}. \tag{122}$$

4.4. The General Case

The dispersion relation (113) is plotted in Figure 10 in the general case. The generalized Jeans wavenumber k_J is given by

$$k_J^2 = \frac{2m^2}{\hbar^2} \left[\sqrt{c_s^4 + \frac{4\pi G \rho \hbar^2}{m^2}} - c_s^2 \right]. \tag{123}$$

It coincides with Equation (103). For $k = k_J$, the perturbation is stationary ($\gamma = 0$). For $k > k_J$, the perturbation decays exponentially rapidly ($\gamma < 0$). The system is stable for these modes. For $k \rightarrow +\infty$, we have $\gamma \sim -\hbar^2 k^4 / 4\zeta m^2$. For $k < k_J$, the perturbation grows exponentially rapidly ($\gamma > 0$). The system is unstable for these modes. For $k = 0$, we have $\gamma = 4\pi G \rho / \zeta$.

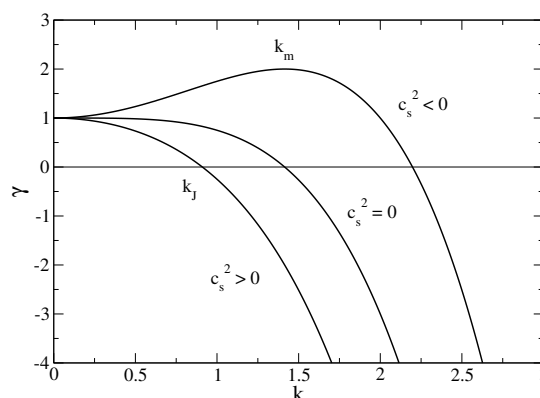


Figure 10. Exponential rate γ for overdamped self-gravitating BECs in the general case. We have normalized the wavenumber by $(4\pi G \rho m^2 / \hbar^2)^{1/4}$, the rate by $4\pi G \rho / \zeta$ and the squared speed of sound by $(4\pi G \rho \hbar^2 / m^2)^{1/2}$. This is equivalent to taking $4\pi G = \rho = m = \hbar = \zeta = 1$ in the dimensional equations. We have selected $c_s^2 = 1, 0, -1$.

For $c_s^2 > 0$, the growth rate is maximum at $k_m = 0$ (infinite wavelength) with $\gamma_{\max} = 4\pi G \rho / \zeta$. For $c_s^2 = 0$, the dispersion relation writes

$$\gamma = -\frac{1}{\zeta} \left(\frac{\hbar^2 k^4}{4m^2} - 4\pi G \rho \right). \tag{124}$$

The quantum Jeans length is given by

$$k_J = \left(\frac{16\pi G\rho m^2}{\hbar^2} \right)^{1/4}. \tag{125}$$

It coincides with Equation (107).

For $c_s^2 < 0$, the growth rate is maximum at

$$k_m = \left(\frac{2m^2|c_s^2|}{\hbar^2} \right)^{1/2} \tag{126}$$

with value

$$\gamma_{\max} = \frac{1}{\xi} \left(\frac{m^2 c_s^4}{\hbar^2} + 4\pi G\rho \right). \tag{127}$$

Since $\gamma_{\max} > 4\pi G\rho/\xi$, an attractive self-interaction increases the growth rate of the Jeans instability.

5. Repulsive or Vanishing Self-Interaction $c_s^2 \geq 0$

We now assume a finite nonzero value of the friction parameter ξ . We first consider the case of a repulsive or vanishing self-interaction corresponding to $c_s^2 \geq 0$.

5.1. The General Case

In this subsection we treat the general case where $\hbar \neq 0$ and $G \neq 0$. Particular cases will be considered in the following subsections. The generalized dispersion relation is given by [61]

$$\omega^2 + i\xi\omega = \frac{\hbar^2 k^4}{4m^2} + c_s^2 k^2 - 4\pi G\rho. \tag{128}$$

This is a second-degree equation for ω whose solutions are

$$\omega = -i\frac{\xi}{2} \pm \sqrt{-\frac{\xi^2}{4} + \frac{\hbar^2 k^4}{4m^2} + c_s^2 k^2 - 4\pi G\rho}. \tag{129}$$

The discriminant

$$\Delta(k) = -\frac{\xi^2}{4} + \frac{\hbar^2 k^4}{4m^2} + c_s^2 k^2 - 4\pi G\rho \tag{130}$$

is a quadratic function of k^2 . It starts from $\Delta(0) = -\xi^2/4 - 4\pi G\rho < 0$ at $k = 0$ and increases monotonically up to $+\infty$. It is negative for $k < k_*$ and positive for $k > k_*$, where the wavenumber k_* is given by

$$k_*^2 = \frac{2m^2}{\hbar^2} \left[\sqrt{c_s^4 + \frac{4\pi G\rho\hbar^2}{m^2} + \frac{\hbar^2 \xi^2}{4m^2}} - c_s^2 \right]. \tag{131}$$

We write the complex pulsation as $\omega = \omega_r + i\gamma$. The perturbation behaves with time as $e^{-i\omega_r t} e^{\gamma t}$, i.e., it oscillates with a pulsation ω_r and evolves exponentially with a rate γ . When $k < k_*$, the real and imaginary parts of the complex pulsation are given by

$$\omega_r = 0, \tag{132}$$

$$\gamma = -\frac{\zeta}{2} \pm \sqrt{\frac{\zeta^2}{4} - \frac{\hbar^2 k^4}{4m^2} - c_s^2 k^2 + 4\pi G\rho}. \tag{133}$$

When $k > k_*$ they are given by

$$\omega_r = \pm \sqrt{-\frac{\zeta^2}{4} + \frac{\hbar^2 k^4}{4m^2} + c_s^2 k^2 - 4\pi G\rho}, \tag{134}$$

$$\gamma = -\frac{\zeta}{2}. \tag{135}$$

The pulsation ω vanishes at the Jeans wavenumber k_J given by [61]

$$k_J^2 = \frac{2m^2}{\hbar^2} \left[\sqrt{c_s^4 + \frac{4\pi G\rho\hbar^2}{m^2}} - c_s^2 \right]. \tag{136}$$

It coincides with the quantum Jeans wavenumber (103) of self-interacting bosons. As already noted in [61] the quantum Jeans length is unaffected by frictional effects. The wavenumber k_* increases with ζ . It is equal to k_J when $\zeta = 0$ and behaves as $k_* \sim (m\zeta/\hbar)^{1/2}$ when $\zeta \rightarrow +\infty$. Therefore $k_J \leq k_*$. For $k > k_*$, the perturbation oscillates with a pulsation ω_r and is damped at a rate $\gamma = -\zeta/2$. For $k_J < k < k_*$, the perturbation evolves exponentially rapidly with a rate γ . The two modes are decaying ($\gamma_+ < 0$ and $\gamma_- < 0$). For $k < k_J$, the perturbation evolves exponentially rapidly with a rate γ . There is a growing mode ($\gamma_+ > 0$) and a decaying mode ($\gamma_- < 0$). The system is stable for the modes $k > k_J$ and unstable for the modes $k < k_J$. We note that the friction ζ has the effect of decreasing the pulsation, increasing the damping rate, and decreasing the growth rate.

The functions ω_r and γ are represented in Figure 11. For $k = 0$:

$$\omega_r = 0, \quad \gamma_+ = -\frac{\zeta}{2} + \sqrt{\frac{\zeta^2}{4} + 4\pi G\rho}, \quad \gamma_- = -\frac{\zeta}{2} - \sqrt{\frac{\zeta^2}{4} + 4\pi G\rho}. \tag{137}$$

For $k = k_J$:

$$\omega_r = 0, \quad \gamma_+ = 0, \quad \gamma_- = -\zeta. \tag{138}$$

For $k = k_*$:

$$\omega_r = 0, \quad \gamma = -\frac{\zeta}{2}. \tag{139}$$

For $k \rightarrow +\infty$:

$$\omega_r \sim \pm \frac{\hbar k^2}{2m}, \quad \gamma = -\frac{\zeta}{2}. \tag{140}$$

The growth rate is maximum at $k_m = 0$ with value $\gamma_{\max} = -\zeta/2 + \sqrt{\zeta^2/4 + 4\pi G\rho}$. For $\zeta = 0$, we have $\gamma_{\max} = \sqrt{4\pi G\rho}$. For $\zeta \rightarrow +\infty$, we have $\gamma_{\max} \sim 4\pi G\rho/\zeta$.

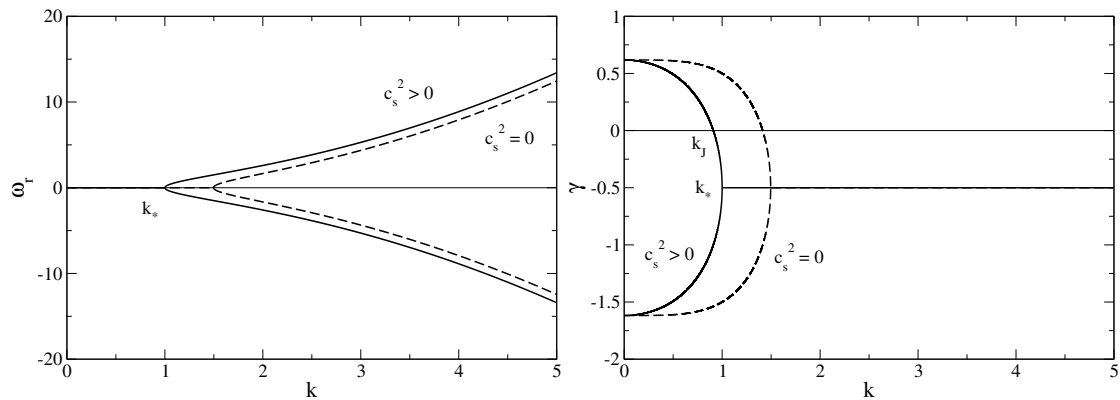


Figure 11. Dispersion relation for self-gravitating BECs in the general case when $c_s^2 \geq 0$. We have normalized the wavenumber by $(4\pi G\rho m^2/\hbar^2)^{1/4}$, the pulsation and the friction by $(4\pi G\rho)^{1/2}$, and the squared speed of sound by $(4\pi G\rho\hbar^2/m^2)^{1/2}$. This is equivalent to taking $4\pi G = \rho = m = \hbar = 1$ in the dimensional equations. We have selected $c_s^2 = 1, 0$ and $\zeta = 1$.

For noninteracting bosons ($c_s = 0$), the preceding discussion remains valid with

$$k_* = \left(\frac{m^2\zeta^2}{\hbar^2} + \frac{16\pi G\rho m^2}{\hbar^2} \right)^{1/4} \tag{141}$$

and

$$k_J = \left(\frac{16\pi G\rho m^2}{\hbar^2} \right)^{1/4}, \tag{142}$$

where k_J coincides with the quantum Jeans wavenumber (107) of noninteracting bosons.

5.2. The Case $G = 0$

The nongravitational limit ($G = 0$) has been studied in [71]. In that case, the generalized dispersion relation (128) reduces to

$$\omega^2 + i\zeta\omega = \frac{\hbar^2 k^4}{4m^2} + c_s^2 k^2, \tag{143}$$

and its solutions are

$$\omega = -i\frac{\zeta}{2} \pm \sqrt{-\frac{\zeta^2}{4} + \frac{\hbar^2 k^4}{4m^2} + c_s^2 k^2}. \tag{144}$$

The discriminant is negative when $k < k_*$ and positive when $k > k_*$, where

$$k_*^2 = \frac{2m^2}{\hbar^2} \left(\sqrt{c_s^4 + \frac{\hbar^2 \zeta^2}{4m^2}} - c_s^2 \right). \tag{145}$$

When $k < k_*$, the real and imaginary parts of the complex pulsation are given by

$$\omega_r = 0, \tag{146}$$

$$\gamma = -\frac{\zeta}{2} \pm \sqrt{\frac{\zeta^2}{4} - \frac{\hbar^2 k^4}{4m^2} - c_s^2 k^2}. \tag{147}$$

When $k > k_*$, they are given by

$$\omega_r = \pm \sqrt{-\frac{\zeta^2}{4} + \frac{\hbar^2 k^4}{4m^2} + c_s^2 k^2}, \tag{148}$$

$$\gamma = -\frac{\zeta}{2}. \tag{149}$$

The wavenumber k_* increases with ζ . It behaves as $k_* \sim \zeta/2c_s$ when $\zeta \rightarrow 0$ and as $k_* \sim (m\zeta/\hbar)^{1/2}$ when $\zeta \rightarrow +\infty$. For $k > k_*$, the perturbation oscillates with a pulsation ω_r and is damped at a rate $\gamma = -\zeta/2$. For $k < k_*$, the perturbation evolves exponentially rapidly with a rate γ . The two modes are decaying ($\gamma_+ < 0$ and $\gamma_- < 0$). The system is stable for all modes.

The functions ω_r and γ are represented in Figure 12. For $k = 0$:

$$\omega_r = 0, \quad \gamma_+ = 0, \quad \gamma_- = -\zeta. \tag{150}$$

For $k = k_*$:

$$\omega_r = 0, \quad \gamma = -\frac{\zeta}{2}. \tag{151}$$

For $k \rightarrow +\infty$:

$$\omega_r \sim \pm \frac{\hbar k^2}{2m}, \quad \gamma = -\frac{\zeta}{2}. \tag{152}$$

For noninteracting bosons ($c_s = 0$), the preceding discussion remains valid with

$$k_* = \left(\frac{m\zeta}{\hbar}\right)^{1/2}. \tag{153}$$

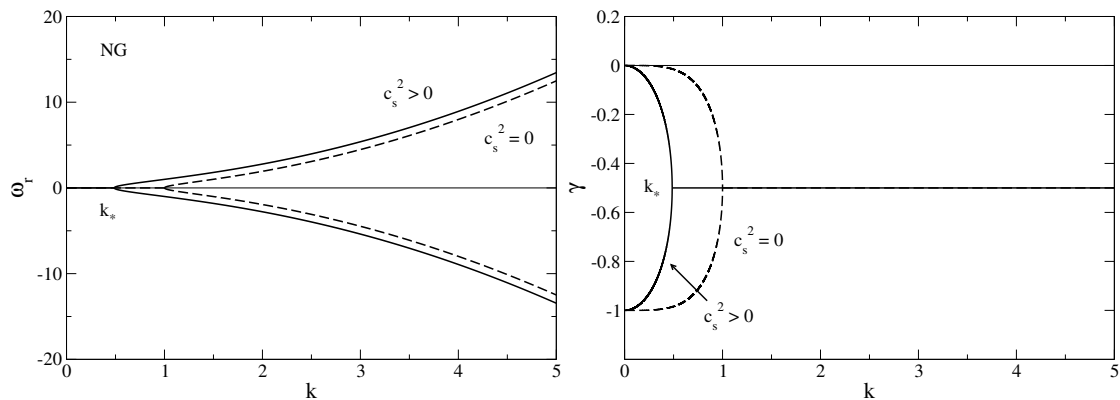


Figure 12. Dispersion relation for BECs in the nongravitational limit ($G = 0$) when $c_s^2 \geq 0$. We have normalized the wavenumber by mc_s/\hbar and the pulsation and the friction by mc_s^2/\hbar . This is equivalent to taking $m = c_s = \hbar = 1$ in the dimensional equations. We have selected $\zeta = 1$. When $c_s = 0$, we can normalize the pulsation by ζ and the wavenumber by $(\zeta m/\hbar)^{1/2}$.

5.3. The Case $\hbar = 0$

The classical (or TF) limit ($\hbar = 0$) has been treated in [85].¹⁷ In that case, the generalized dispersion relation (128) reduces to

$$\omega^2 + i\zeta\omega = c_s^2 k^2 - 4\pi G\rho, \tag{154}$$

and its solutions are

$$\omega = -i\frac{\zeta}{2} \pm \sqrt{-\frac{\zeta^2}{4} + c_s^2 k^2 - 4\pi G\rho}. \tag{155}$$

The discriminant is negative when $k < k_*$ and positive when $k > k_*$, where

$$k_* = \left(\frac{4\pi G\rho}{c_s^2} + \frac{\zeta^2}{4c_s^2} \right)^{1/2}. \tag{156}$$

When $k < k_*$, the real and imaginary parts of the complex pulsation are given by

$$\omega_r = 0, \tag{157}$$

$$\gamma = -\frac{\zeta}{2} \pm \sqrt{\frac{\zeta^2}{4} - c_s^2 k^2 + 4\pi G\rho}. \tag{158}$$

When $k > k_*$, they are given by

$$\omega_r = \pm \sqrt{-\frac{\zeta^2}{4} + c_s^2 k^2 - 4\pi G\rho}, \tag{159}$$

$$\gamma = -\frac{\zeta}{2}. \tag{160}$$

The pulsation ω vanishes at the Jeans wavenumber

$$k_J = \left(\frac{4\pi G\rho}{c_s^2} \right)^{1/2}. \tag{161}$$

It coincides with the classical (or TF) Jeans wavenumber (90). The wavenumber k_* increases with ζ . It is equal to k_J when $\zeta = 0$ and behaves as $k_* \sim \zeta/2c_s$ when $\zeta \rightarrow +\infty$. Therefore $k_J \leq k_*$. For $k > k_*$, the perturbation oscillates with a pulsation ω_r and is damped at a rate $\gamma = -\zeta/2$. For $k_J < k < k_*$, the perturbation evolves exponentially rapidly with a rate γ . The two modes are decaying ($\gamma_+ < 0$ and $\gamma_- < 0$). For $k < k_J$, the perturbation evolves exponentially rapidly with a rate γ . There is a growing mode ($\gamma_+ > 0$) and a decaying mode ($\gamma_- < 0$). The system is stable for the modes $k > k_J$ and unstable for the modes $k < k_J$.

The functions ω_r and γ are represented in Figure 13. The results from Equations (137)–(140) remain valid except that $\omega_r \sim \pm c_s k$ for $k \rightarrow +\infty$.

¹⁷ This study was done in relation to the chemotaxis of bacterial populations based on the Keller–Segel [86] model.

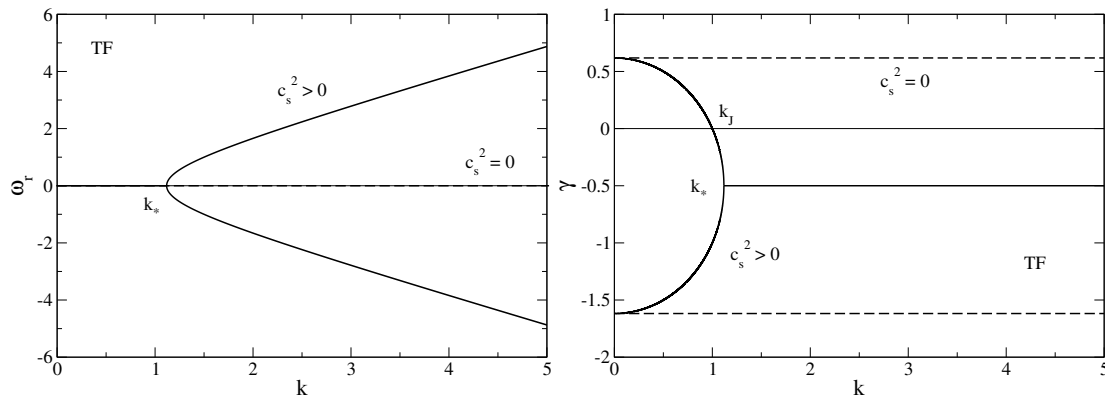


Figure 13. Dispersion relation for self-gravitating BECs in the TF limit ($\hbar = 0$) when $c_s^2 \geq 0$. We have normalized the wavenumber by $(4\pi G\rho/c_s^2)^{1/2}$ and the pulsation and the friction by $(4\pi G\rho)^{1/2}$. This is equivalent to taking $4\pi G = \rho = m = c_s = 1$ in the dimensional equations. We have selected $\xi = 1$. When $c_s = 0$, we can normalize the pulsation by ξ and the density by $\xi^2/4\pi G$.

For noninteracting bosons ($c_s = 0$), the discriminant is always negative and the solution of the dispersion relation is

$$\omega_r = 0 \quad \text{and} \quad \gamma = -\frac{\xi}{2} \pm \sqrt{\frac{\xi^2}{4} + 4\pi G\rho}. \tag{162}$$

The perturbation evolves exponentially rapidly with a rate γ which is independent of k . There is a growing mode ($\gamma_+ > 0$) and a decaying mode ($\gamma_- < 0$). The system is unstable for all modes ($k_*, k_J \rightarrow +\infty$).

5.4. The Case $\hbar = G = 0$

In the classical (or TF) + nongravitational limit ($\hbar = G = 0$) the generalized dispersion relation (128) reduces to

$$\omega^2 + i\xi\omega = c_s^2 k^2, \tag{163}$$

and its solutions are

$$\omega = -i\frac{\xi}{2} \pm \sqrt{-\frac{\xi^2}{4} + c_s^2 k^2}. \tag{164}$$

The discriminant is negative when $k < k_*$ and positive when $k > k_*$, where

$$k_* = \frac{\xi}{2c_s}. \tag{165}$$

When $k < k_*$, the real and imaginary parts of the complex pulsation are given by

$$\omega_r = 0, \tag{166}$$

$$\gamma = -\frac{\xi}{2} \pm \sqrt{\frac{\xi^2}{4} - c_s^2 k^2}. \tag{167}$$

When $k > k_*$, they are given by

$$\omega_r = \pm \sqrt{-\frac{\xi^2}{4} + c_s^2 k^2}, \tag{168}$$

$$\gamma = -\frac{\zeta}{2}. \tag{169}$$

For $k > k_*$, the perturbation oscillates with a pulsation ω_r and is damped at a rate $\gamma = -\zeta/2$. For $k < k_*$, the perturbation evolves exponentially rapidly with a rate γ . The two modes are decaying ($\gamma_+ < 0$ and $\gamma_- < 0$). The system is stable for all modes.

The functions ω_r and γ are represented in Figure 14. The results from Equations (150)–(152) remain valid except that $\omega_r \sim \pm c_s k$ for $k \rightarrow +\infty$.

For noninteracting bosons ($c_s = 0$), the solutions of the dispersion relation reduce to $\omega_r = 0$, $\gamma_+ = 0$ and $\gamma_- = -\zeta$.

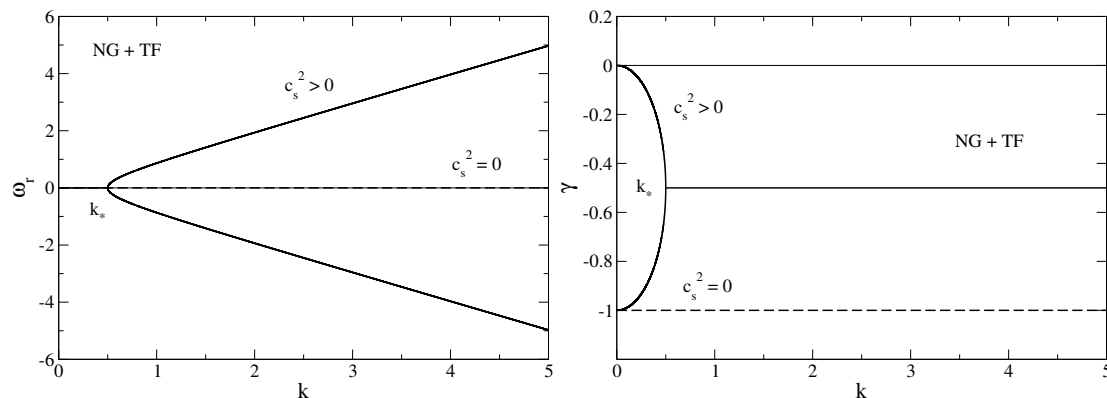


Figure 14. Dispersion relation for BECs in the nongravitational + TF limit ($G = \hbar = 0$) when $c_s^2 \geq 0$. We have normalized the wavenumber by ζ/c_s and the pulsation by ζ . This is equivalent to taking $\zeta = c_s = 1$ in the dimensional equations.

6. Attractive Self-Interaction $c_s^2 < 0$

As in the previous section, we assume a finite nonzero value of the friction parameter ζ but we now consider the case of an attractive self-interaction corresponding to $c_s^2 < 0$.

6.1. The General Case

In this subsection we treat the general case where $\hbar \neq 0$ and $G \neq 0$. Particular cases will be considered in the following subsections. The generalized dispersion relation is given by [61]

$$\omega^2 + i\zeta\omega = \frac{\hbar^2 k^4}{4m^2} - |c_s^2|k^2 - 4\pi G\rho. \tag{170}$$

This is a second-degree equation for ω whose solutions are

$$\omega = -i\frac{\zeta}{2} \pm \sqrt{-\frac{\zeta^2}{4} + \frac{\hbar^2 k^4}{4m^2} - |c_s^2|k^2 - 4\pi G\rho}. \tag{171}$$

The discriminant

$$\Delta(k) = -\frac{\zeta^2}{4} + \frac{\hbar^2 k^4}{4m^2} - |c_s^2|k^2 - 4\pi G\rho \tag{172}$$

is a quadratic function of k^2 . It starts from $\Delta(0) = -\zeta^2/4 - 4\pi G\rho < 0$ at $k = 0$, decreases, reaches a minimum value

$$\Delta_{\min} = -\frac{\zeta^2}{4} - \frac{m^2 c_s^4}{\hbar^2} - 4\pi G\rho \quad \text{at} \quad k_m = \left(\frac{2m^2 |c_s^2|}{\hbar^2} \right)^{1/2}, \tag{173}$$

and increases up to $+\infty$. The critical wavenumber k_m is independent of ξ and coincides with Equation (110). The discriminant is negative when $k < k_*$ and positive when $k > k_*$, where the wavenumber k_* is given by

$$k_*^2 = \frac{2m^2}{\hbar^2} \left[\sqrt{c_s^4 + \frac{\hbar^2 4\pi G\rho}{m^2} + \frac{\hbar^2 \xi^2}{4m^2}} + |c_s^2| \right]. \tag{174}$$

We write the complex pulsation as $\omega = \omega_r + i\gamma$. The perturbation behaves with time as $e^{-i\omega_r t} e^{\gamma t}$, i.e., it oscillates with a pulsation ω_r and evolves exponentially with a rate γ . When $k < k_*$, the real and imaginary parts of the complex pulsation are given by

$$\omega_r = 0, \tag{175}$$

$$\gamma = -\frac{\xi}{2} \pm \sqrt{\frac{\xi^2}{4} - \frac{\hbar^2 k^4}{4m^2} + |c_s^2| k^2 + 4\pi G\rho}. \tag{176}$$

When $k > k_*$, they are given by

$$\omega_r = \pm \sqrt{-\frac{\xi^2}{4} + \frac{\hbar^2 k^4}{4m^2} - |c_s^2| k^2 - 4\pi G\rho}, \tag{177}$$

$$\gamma = -\frac{\xi}{2}. \tag{178}$$

The pulsation ω vanishes at the Jeans wavenumber k_J given by [61]

$$k_J^2 = \frac{2m^2}{\hbar^2} \left[\sqrt{c_s^4 + \frac{\hbar^2 4\pi G\rho}{m^2}} + |c_s^2| \right]. \tag{179}$$

It is unaffected by frictional effects and coincides with the quantum Jeans wavenumber (103) of self-interacting bosons. The wavenumber k_* increases with ξ . It is equal to k_J when $\xi = 0$ and behaves as $k_* \sim (m\xi/\hbar)^{1/2}$ when $\xi \rightarrow +\infty$. Therefore $k_m \leq k_J \leq k_*$. For $k > k_*$, the perturbation oscillates with a pulsation ω_r and is damped at a rate $\gamma = -\xi/2$. For $k_J < k < k_*$, the perturbation evolves exponentially rapidly with a rate γ . The two modes are decaying ($\gamma_+ < 0$ and $\gamma_- < 0$). For $k < k_J$, the perturbation evolves exponentially rapidly with a rate γ . There is a growing mode ($\gamma_+ > 0$) and a decaying mode ($\gamma_- < 0$). The system is stable for the modes $k > k_J$ and unstable for the modes $k < k_J$. We note that the friction ξ has the effect of decreasing the pulsation, increasing the damping rate, and decreasing the growth rate.

The functions ω_r and γ are represented in Figure 15. The results from Equations (137)–(140) remain valid. The growth rate is maximum at $k = k_m$ with value

$$\gamma_{\max} = -\frac{\xi}{2} + \sqrt{\frac{\xi^2}{4} + \frac{m^2 c_s^4}{\hbar^2} + 4\pi G\rho}. \tag{180}$$

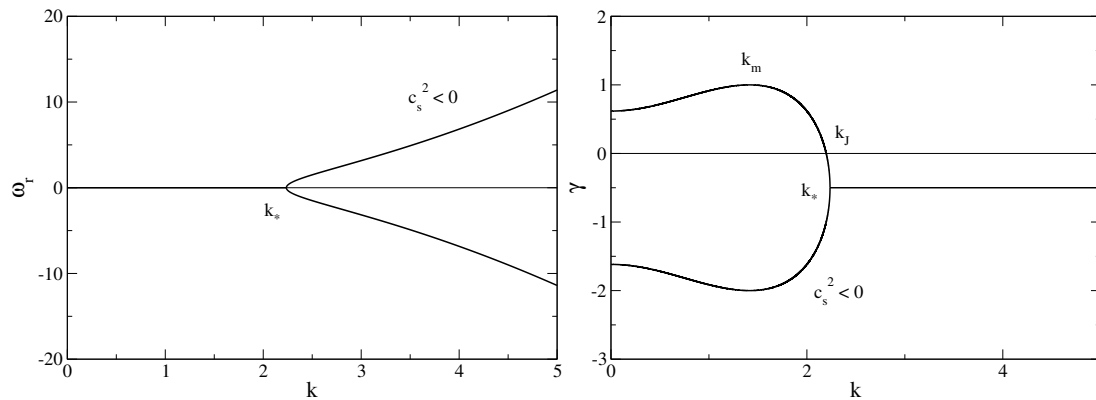


Figure 15. Dispersion relation for self-gravitating BECs in the general case when $c_s^2 < 0$. We have normalized the wavenumber by $(4\pi G\rho m^2/\hbar^2)^{1/4}$, the pulsation and the friction by $(4\pi G\rho)^{1/2}$, and the squared speed of sound by $(4\pi G\rho\hbar^2/m^2)^{1/2}$. This is equivalent to taking $4\pi G = \rho = m = \hbar = 1$ in the dimensional equations. We have selected $c_s^2 = -1$ and $\zeta = 1$.

6.2. The Case $G = 0$

The nongravitational limit ($G = 0$) has been studied in [71]. In that case, the generalized dispersion relation (170) reduces to

$$\omega^2 + i\zeta\omega = \frac{\hbar^2 k^4}{4m^2} - |c_s^2|k^2, \tag{181}$$

and its solutions are

$$\omega = -i\frac{\zeta}{2} \pm \sqrt{-\frac{\zeta^2}{4} + \frac{\hbar^2 k^4}{4m^2} - |c_s^2|k^2}. \tag{182}$$

The discriminant is negative when $k < k_*$ and positive when $k > k_*$, where

$$k_*^2 = \frac{2m^2}{\hbar^2} \left(\sqrt{c_s^4 + \frac{\hbar^2 \zeta^2}{4m^2}} + |c_s^2| \right). \tag{183}$$

When $k < k_*$, the real and imaginary parts of the complex pulsation are given by

$$\omega_r = 0, \tag{184}$$

$$\gamma = -\frac{\zeta}{2} \pm \sqrt{\frac{\zeta^2}{4} - \frac{\hbar^2 k^4}{4m^2} + |c_s^2|k^2}. \tag{185}$$

When $k > k_*$, they are given by

$$\omega_r = \pm \sqrt{-\frac{\zeta^2}{4} + \frac{\hbar^2 k^4}{4m^2} - |c_s^2|k^2}, \tag{186}$$

$$\gamma = -\frac{\zeta}{2}. \tag{187}$$

The pulsation vanishes at the effective Jeans wavenumber

$$k_J = \left(\frac{4m^2|c_s^2|}{\hbar^2} \right)^{1/2}. \tag{188}$$

It is unaffected by frictional effects and coincides with Equation (98). The wavenumber k_* increases with ξ . It is equal to k_J when $\xi = 0$ and behaves as $k_* \sim (m\xi/\hbar)^{1/2}$ when $\xi \rightarrow +\infty$. Therefore $k_m \leq k_J \leq k_*$. For $k > k_*$, the perturbation oscillates with a pulsation ω_r and is damped at a rate $\gamma = -\xi/2$. For $k_J < k < k_*$, the perturbation evolves exponentially rapidly with a rate γ . The two modes are decaying ($\gamma_+ < 0$ and $\gamma_- < 0$). For $k < k_J$, the perturbation evolves exponentially rapidly with a rate γ . There is a growing mode ($\gamma_+ > 0$) and a decaying mode ($\gamma_- < 0$). The system is stable for the modes $k > k_J$ and unstable for the modes $k < k_J$.

The functions ω_r and γ are represented in Figure 16. The results from Equations (137)–(140) remain valid. The growth rate is maximum at

$$k_m = \left(\frac{2m^2|c_s^2|}{\hbar^2} \right)^{1/2} \tag{189}$$

with value

$$\gamma_{\max} = -\frac{\xi}{2} + \sqrt{\frac{\xi^2}{4} + \frac{m^2c_s^4}{\hbar^2}}. \tag{190}$$

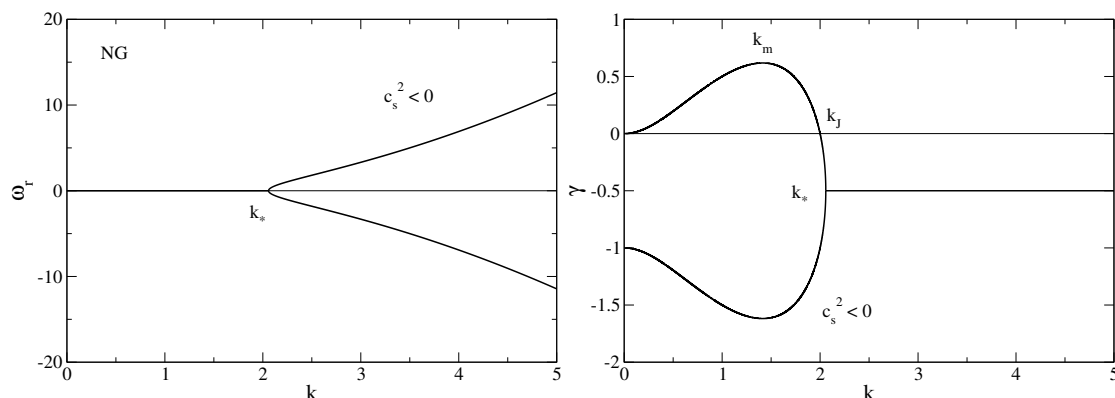


Figure 16. Dispersion relation for BECs in the nongravitational limit ($G = 0$) when $c_s^2 < 0$. We have normalized the wavenumber by $(m^2|c_s^2|/\hbar^2)^{1/2}$ and the pulsation and the friction by $m|c_s^2|/\hbar$. This is equivalent to taking $m = |c_s^2| = \hbar = 1$ in the dimensional equations. We have selected $\xi = 1$.

6.3. The Case $\hbar = 0$

In the classical (or TF) limit ($\hbar = 0$), the generalized dispersion relation (170) reduces to

$$\omega^2 + i\xi\omega = -|c_s^2|k^2 - 4\pi G\rho, \tag{191}$$

and its solutions are

$$\omega = -i\frac{\xi}{2} \pm \sqrt{-\frac{\xi^2}{4} - |c_s^2|k^2 - 4\pi G\rho}. \tag{192}$$

The discriminant is always negative. The real and imaginary parts of the complex pulsation are given by

$$\omega_r = 0, \tag{193}$$

$$\gamma = -\frac{\xi}{2} \pm \sqrt{\frac{\xi^2}{4} + |c_s^2|k^2 + 4\pi G\rho}. \tag{194}$$

The perturbation evolves exponentially rapidly with a rate γ . There is a growing mode ($\gamma_+ > 0$) and a decaying mode ($\gamma_- < 0$). The system is unstable for all modes ($k_*, k_J \rightarrow +\infty$).

The functions ω_r and γ are represented in Figure 17. For $k = 0$:

$$\gamma = -\frac{\xi}{2} \pm \sqrt{\frac{\xi^2}{4} + 4\pi G\rho}. \tag{195}$$

For $k \rightarrow +\infty$:

$$\gamma = \pm |c_s^2|^{1/2}k. \tag{196}$$

The growth rate tends to $+\infty$ when $k \rightarrow +\infty$.

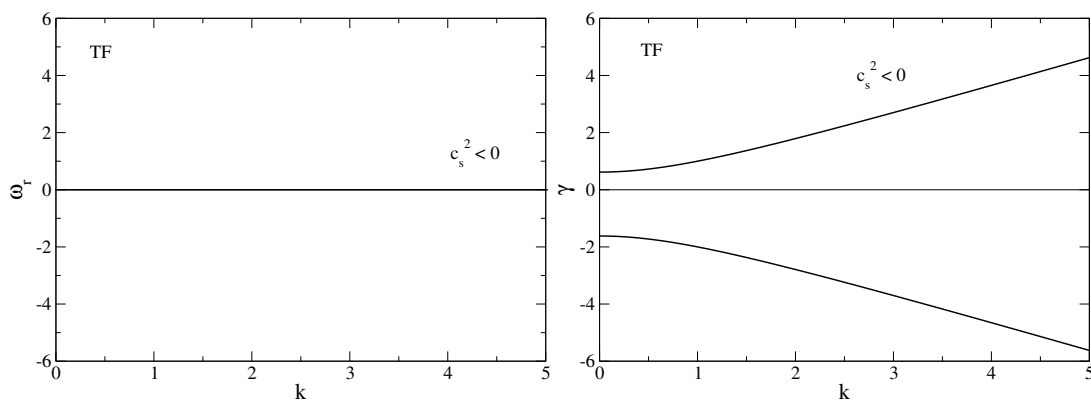


Figure 17. Dispersion relation for self-gravitating BECs in the TF limit ($\hbar = 0$) when $c_s^2 < 0$. We have normalized the wavenumber by $(4\pi G\rho/|c_s^2|)^{1/2}$ and the pulsation and the friction by $(4\pi G\rho)^{1/2}$. This is equivalent to taking $4\pi G = \rho = m = |c_s^2| = 1$ in the dimensional equations. We have selected $\xi = 1$.

6.4. The Case $\hbar = G = 0$

In the classical (or TF) + nongravitational limit ($\hbar = G = 0$) the generalized dispersion relation (170) reduces to

$$\omega^2 + i\xi\omega = -|c_s^2|k^2, \tag{197}$$

and its solutions are

$$\omega = -i\frac{\xi}{2} \pm \sqrt{-\frac{\xi^2}{4} - |c_s^2|k^2}. \tag{198}$$

The discriminant is always negative. The real and imaginary parts of the complex pulsation are given by

$$\omega_r = 0, \tag{199}$$

$$\gamma = -\frac{\xi}{2} \pm \sqrt{\frac{\xi^2}{4} + |c_s^2|k^2}. \tag{200}$$

The perturbation evolves exponentially rapidly with a rate γ . There is a growing mode ($\gamma_+ > 0$) and a decaying mode ($\gamma_- < 0$). The system is unstable for all modes ($k_*, k_J \rightarrow +\infty$).

The functions ω_r and γ are represented in Figure 18. For $k = 0$:

$$\gamma_+ = 0, \quad \gamma_- = -\zeta. \tag{201}$$

For $k \rightarrow +\infty$:

$$\gamma = \pm |c_s^2|^{1/2} k. \tag{202}$$

The growth rate tends to $+\infty$ when $k \rightarrow +\infty$.

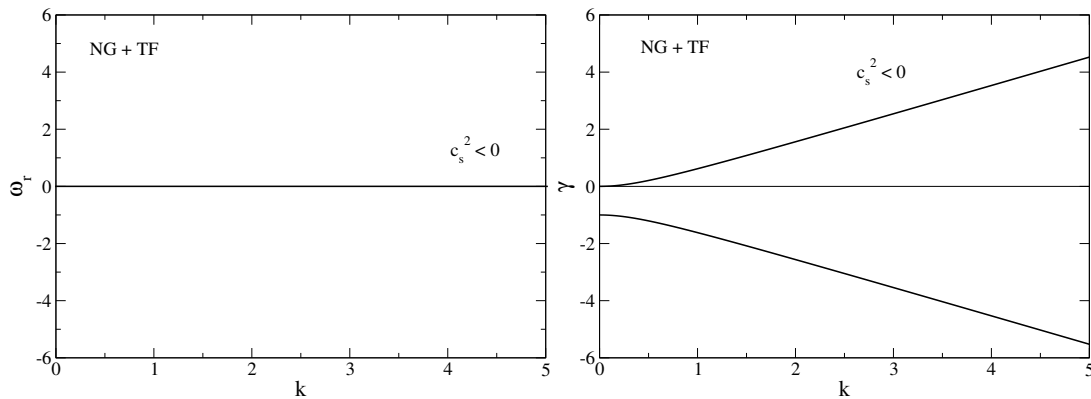


Figure 18. Dispersion relation for BECs in the nongravitational and TF limit ($G = \hbar = 0$) when $c_s^2 < 0$. We have normalized the wavenumber by $\zeta/|c_s^2|^{1/2}$ and the pulsation by ζ . This is equivalent to taking $\zeta = |c_s^2| = 1$ in the dimensional equations.

7. Summary and Discussion

In this section, we summarize the results obtained previously.

7.1. The Case $c_s^2 > 0$

When ζ is finite and nonzero, the perturbation undergoes damped oscillations for $k > k_*$, decays exponentially rapidly for $k_J < k < k_*$, and grows exponentially rapidly for $k < k_J$ (see Figure 11). The growth rate is maximum at $k_m = 0$ (infinite wavelength). When $\hbar = 0$ (see Figure 13), the situation is the same. When $G = 0$ (see Figure 12), there is no instability ($k_J = 0$). In that case, the perturbation undergoes damped oscillations for $k > k_*$ and decays exponentially rapidly for $k < k_*$. When $G = \hbar = 0$ (see Figure 14), the situation is the same.

When $\zeta = 0$, in which case $k_* = k_J$, the perturbation oscillates for $k > k_J$ and grows exponentially rapidly for $k < k_J$ (see Figure 5). The growth rate is maximum at $k_m = 0$ (infinite wavelength). When $\hbar = 0$ (see Figure 3), the situation is the same. When $G = 0$ (see Figure 4), there is no instability ($k_J = 0$). In that case, the perturbation oscillates for all k . When $G = \hbar = 0$ (see Figure 2), the situation is the same.

When $\zeta \rightarrow +\infty$, in which case $k_* \rightarrow +\infty$, the perturbation decays exponentially rapidly for $k > k_J$ and grows exponentially rapidly for $k < k_J$ (see Figure 10). The growth rate is maximum at $k_m = 0$ (infinite wavelength). When $\hbar = 0$ (see Figure 8), the situation is the same. When $G = 0$ (see Figure 9), there is no instability ($k_J = 0$). In that case, the perturbation decays exponentially rapidly for all k . When $G = \hbar = 0$ (see Figure 7), the situation is the same.

7.2. The Case $c_s^2 = 0$

When ζ is finite and nonzero, the perturbation undergoes damped oscillations for $k > k_*$, decays exponentially rapidly for $k_J < k < k_*$, and grows exponentially rapidly for $k < k_J$ (see Figure 11). The growth rate is maximum at $k_m = 0$ (infinite wavelength). When $\hbar = 0$ (see Figure 13), there is nothing to prevent the instability ($k_J, k_* \rightarrow +\infty$). The perturbation grows

exponentially rapidly for all k with the same rate. When $G = 0$ (see Figure 12), there is no instability ($k_J = 0$). In that case, the perturbation undergoes damped oscillations for $k > k_*$ and decays exponentially rapidly for $k < k_*$. When $\hbar = G = 0$ (see Figure 14), the perturbation is stationary ($k_J = 0$ and $k_* \rightarrow +\infty$).

When $\xi = 0$, in which case $k_* = k_J$, the perturbation oscillates for $k > k_J$ and grows exponentially rapidly for $k < k_J$ (see Figure 5). The growth rate is maximum at $k_m = 0$ (infinite wavelength). When $\hbar = 0$ (see Figure 3), there is nothing to prevent the instability ($k_J \rightarrow +\infty$). The perturbation grows exponentially rapidly for all k with the same rate. When $G = 0$ (see Figure 4), there is no instability ($k_J = 0$). In that case, the perturbation oscillates for all k . When $\hbar = G = 0$ (see Figure 2), the perturbation is stationary.

When $\xi \rightarrow +\infty$, in which case $k_* \rightarrow +\infty$, the perturbation decays exponentially rapidly for $k > k_J$ and grows exponentially rapidly for $k < k_J$ (see Figure 10). The growth rate is maximum at $k_m = 0$ (infinite wavelength). When $\hbar = 0$ (see Figure 8), there is nothing to prevent the instability ($k_J \rightarrow +\infty$). The perturbation grows exponentially rapidly for all k with the same rate. When $G = 0$ (see Figure 9), there is no instability ($k_J = 0$). In that case, the perturbation decays exponentially rapidly for all k . When $\hbar = G = 0$ (see Figure 7), the perturbation is stationary.

7.3. The Case $c_s^2 < 0$

When ξ is finite and nonzero, the perturbation undergoes damped oscillations for $k > k_*$, decays exponentially rapidly for $k_J < k < k_*$, and grows exponentially rapidly for $k < k_J$ (see Figure 15). The growth rate is maximum at $k_m > 0$. When $G = 0$ (see Figure 16), the situation is the same. When $\hbar = 0$ (see Figure 17), there is nothing to prevent the instability ($k_J, k_* \rightarrow +\infty$). In that case, the perturbation grows exponentially rapidly for all k and the growth rate is infinite for $k \rightarrow +\infty$ (zero wavelength). When $\hbar = G = 0$ (see Figure 18), the situation is the same.

When $\xi = 0$, in which case $k_* = k_J$, the perturbation oscillates for $k > k_J$ and grows exponentially rapidly for $k < k_J$ (see Figure 5). The growth rate is maximum at $k_m > 0$. When $G = 0$ (see Figure 4), the situation is the same. When $\hbar = 0$ (see Figure 3), there is nothing to prevent the instability ($k_J \rightarrow +\infty$). In that case, the perturbation grows exponentially rapidly for all k and the growth rate is infinite for $k \rightarrow +\infty$ (zero wavelength). When $\hbar = G = 0$ (see Figure 2), the situation is the same.

When $\xi \rightarrow +\infty$, in which case $k_* \rightarrow +\infty$, the perturbation decays exponentially rapidly for $k > k_J$ and grows exponentially rapidly for $k < k_J$ (see Figure 10). The growth rate is maximum at $k_m > 0$. When $G = 0$ (see Figure 9), the situation is the same. When $\hbar = 0$ (see Figure 8), there is nothing to prevent the instability ($k_J \rightarrow +\infty$). In that case, the perturbation grows exponentially rapidly for all k and the growth rate is infinite for $k \rightarrow +\infty$ (zero wavelength). When $\hbar = G = 0$ (see Figure 7), the situation is the same.

8. Conclusions

In this paper, we have made an exhaustive study of the Jeans instability of an infinite homogeneous dissipative self-gravitating BEC based on the generalized GPP equations introduced in [61]. Following our previous works [28,52], we have considered the case of an arbitrary (vanishing, repulsive or attractive) self-interaction. The general expression of the Jeans wavenumber is given by Equation (45). Self-gravitating BECs with a vanishing or a repulsive self-interaction are only subject to the gravitational instability. The Jeans length is due to the interplay between the quantum pressure (Heisenberg), the repulsive self-interaction and the self-gravity. Self-gravitating BECs with an attractive self-interaction can experience, in addition, a hydrodynamical (tachyonic) instability. In that case, the Jeans length is due to the interplay between the quantum pressure (Heisenberg), the attractive self-interaction and the self-gravity. This hydrodynamical instability exists even in the absence of gravitation. As shown in our previous work [28], the maximum growth rate of the hydrodynamical or gravito-hydrodynamical instability occurs at a finite wavelength λ_m while the maximum growth rate of the purely gravitational instability occurs at an infinite wavelength, and the

value of the maximum growth rate is smaller. We have studied how the dissipation affects the results obtained in [28]. Generically, in the absence of friction ($\xi = 0$), the perturbation oscillates for $\lambda < \lambda_J$ and grows exponentially rapidly for $\lambda > \lambda_J$. With the friction, a new scale $\lambda_* < \lambda_J$ appears in the problem. The perturbation undergoes damped oscillations for $\lambda < \lambda_*$, decays exponentially rapidly for $\lambda_* < \lambda < \lambda_J$, and grows exponentially rapidly for $\lambda > \lambda_J$. In the overdamped limit ($\xi \rightarrow +\infty$), the perturbation decays exponentially rapidly for $\lambda < \lambda_J$ and grows exponentially rapidly for $\lambda > \lambda_J$. As already shown in [61], the Jeans length is not affected by the friction. The effect of the friction is to damp the perturbation in the stable regime ($\lambda < \lambda_J$), to diminish the pulsation in the range $\lambda < \lambda_*$ (where the damping rate is constant), to increase the damping rate $|\gamma_-|$ in the range $\lambda < \lambda_J$, and to diminish the growth rate γ_+ in the range $\lambda > \lambda_J$. We have considered specific situations of physical interest: the noninteracting limit ($a_s = 0$), the nongravitational limit ($G = 0$), and the TF limit ($\hbar = 0$). In the present paper, we have developed a general formalism to treat the Jeans instability of a dissipative quantum fluid. The case of a standard BEC can be obtained from our general formalism by replacing the squared speed of sound c_s^2 by its expression given by Equation (24). The case of fermions can be treated similarly by using the results of Section 2.6. The corresponding Jeans mass M_J and Jeans length λ_J have been given in [28] and their numerical values for different types of bosonic and fermionic DM particles in a cosmological context have been calculated in [52]. In a forthcoming paper [65], we shall complete the studies initiated in [28,52] in the light of the present results.

Funding: This research received no external funding.

Conflicts of Interest: The author declares no conflict of interest.

Appendix A. Thermodynamical Identities

In this Appendix, we recall basic elements of thermodynamics and apply them to BECs at absolute zero temperature (see [61] for a more detailed discussion).

The first principle of thermodynamics can be written as

$$d\left(\frac{u}{\rho}\right) = -Pd\left(\frac{1}{\rho}\right) + Td\left(\frac{s}{\rho}\right), \tag{A1}$$

where u is the density of internal energy, s is the density of entropy, ρ is the mass density, and P is the pressure. For a cold ($T = 0$) gas, it reduces to

$$d\left(\frac{u}{\rho}\right) = -Pd\left(\frac{1}{\rho}\right) = \frac{P}{\rho^2}d\rho. \tag{A2}$$

Introducing the enthalpy per particle

$$h = \frac{P + u}{\rho}, \tag{A3}$$

we get

$$du = hd\rho \quad \text{and} \quad dh = \frac{dP}{\rho}. \tag{A4}$$

Comparing Equation (A3) with the Gibbs–Duhem relation at $T = 0$:

$$u = -P + Ts + \frac{\mu}{m}\rho \quad \Rightarrow \quad \frac{\mu}{m} = \frac{P + u}{\rho}, \tag{A5}$$

we see that the enthalpy h is equal to the chemical potential μ by unit of mass: $h = \mu/m$. For a barotropic gas, for which $P = P(\rho)$, the foregoing equations can be written as

$$P(\rho) = -\frac{d(u/\rho)}{d(1/\rho)} = \rho^2 \left[\frac{u(\rho)}{\rho} \right]' = \rho u'(\rho) - u(\rho) \quad \Rightarrow \quad P'(\rho) = \rho u''(\rho), \tag{A6}$$

and

$$h(\rho) = \frac{P(\rho) + u(\rho)}{\rho}, \quad h(\rho) = u'(\rho), \quad h'(\rho) = \frac{P'(\rho)}{\rho}. \tag{A7}$$

Comparing Equation (A6) with Equation (19), we see that the potential $V(\rho)$ represents the density of internal energy

$$u(\rho) = V(\rho). \tag{A8}$$

We then have

$$h(\rho) = \frac{P(\rho) + V(\rho)}{\rho}, \quad h(\rho) = V'(\rho), \quad h'(\rho) = \frac{P'(\rho)}{\rho}. \tag{A9}$$

In particular, we see that the enthalpy is equal to the first derivative of the potential V .

Appendix B. Generalized Wave Equation

In this Appendix, we briefly recall the derivation of the generalized Schrödinger Equation (4) given in [71] from the formalism of scale relativity [63].

Nottale [63] has shown that the standard Schrödinger equation is equivalent to the fundamental equation of dynamics

$$\frac{DU}{Dt} = -\nabla\Phi, \tag{A10}$$

where $\mathbf{F} = -\nabla\Phi$ is the force by unit of mass exerted on a particle, provided that $\mathbf{U}(\mathbf{r}, t)$ is interpreted as a complex velocity field and D/Dt as a complex time derivative operator (or covariant derivative) defined by

$$\frac{D}{Dt} = \frac{\partial}{\partial t} + \mathbf{U} \cdot \nabla - i\mathcal{D}\Delta, \tag{A11}$$

where

$$\mathcal{D} = \frac{\hbar}{2m} \tag{A12}$$

is the Nelson [87] diffusion coefficient of quantum mechanics or the fractal fluctuation parameter in the theory of scale relativity [63]. In Ref. [71] we proposed to generalize this procedure by including a dissipative term in the fundamental equation of dynamics. Specifically, we considered an equation of motion of the form

$$\frac{DU}{Dt} = -\nabla\Phi - \text{Re}(\gamma\mathbf{U}) \tag{A13}$$

involving a linear friction force $-\gamma\mathbf{U}$, where γ is a complex friction coefficient.¹⁸ Using the expression (A11) of the covariant derivative, Equation (A13) can be rewritten as a damped complex viscous Burgers equation

$$\frac{\partial\mathbf{U}}{\partial t} + (\mathbf{U} \cdot \nabla)\mathbf{U} = i\mathcal{D}\Delta\mathbf{U} - \nabla\Phi - \text{Re}(\gamma\mathbf{U}) \tag{A14}$$

¹⁸ As explained in [71], it is necessary to take the real part of the complex friction force in Equation (A13) in order to guarantee the local conservation of the normalization condition.

with an imaginary viscosity $\nu = i\mathcal{D}$ and a complex friction γ . It can be shown [63] that the complex velocity field can be written as the gradient of a complex action:

$$\mathbf{U} = \frac{\nabla \mathcal{S}}{m}. \tag{A15}$$

This defines a potential flow. As a consequence, the flow is irrotational: $\nabla \times \mathbf{U} = \mathbf{0}$. Using the well-known identities of fluid mechanics $(\mathbf{U} \cdot \nabla)\mathbf{U} = \nabla(\mathbf{U}^2/2) - \mathbf{U} \times (\nabla \times \mathbf{U})$ and $\Delta \mathbf{U} = \nabla(\nabla \cdot \mathbf{U}) - \nabla \times (\nabla \times \mathbf{U})$ which reduce to $(\mathbf{U} \cdot \nabla)\mathbf{U} = \nabla(\mathbf{U}^2/2)$ and $\Delta \mathbf{U} = \nabla(\nabla \cdot \mathbf{U})$ for an irrotational flow, and using the identity $\nabla \cdot \mathbf{U} = \Delta \mathcal{S}/m$ resulting from Equation (A15), we find that Equation (A13) is equivalent to the complex quantum Hamilton–Jacobi (or Bernoulli) equation

$$\frac{\partial \mathcal{S}}{\partial t} + \frac{1}{2m}(\nabla \mathcal{S})^2 - i\mathcal{D}\Delta \mathcal{S} + m\Phi + V(t) + \text{Re}(\gamma \mathcal{S}) = 0, \tag{A16}$$

where $V(t)$ is a “constant” of integration that may depend on time. We now define the wave function $\psi(\mathbf{r}, t)$ through the complex Cole–Hopf transformation

$$\mathcal{S} = -2im\mathcal{D} \ln \psi, \tag{A17}$$

which is equivalently to the WKB formula

$$\psi = e^{i\mathcal{S}/\hbar}. \tag{A18}$$

Substituting Equation (A17) into Equation (A16), and using the identity

$$\Delta(\ln \psi) = \frac{\Delta \psi}{\psi} - \frac{1}{\psi^2}(\nabla \psi)^2, \tag{A19}$$

we obtain the generalized Schrödinger equation [71]

$$i\hbar \frac{\partial \psi}{\partial t} = -\frac{\hbar^2}{2m}\Delta \psi + m\Phi \psi + V\psi + \hbar \text{Im}(\gamma \ln \psi)\psi. \tag{A20}$$

Writing $\gamma = \gamma_R + i\gamma_I$, where γ_R is the classical friction coefficient and γ_I is the quantum friction coefficient, and using the identity

$$\text{Im}(\gamma \ln \psi) = \gamma_I \ln |\psi| - \frac{1}{2}i\gamma_R \ln \left(\frac{\psi}{\psi^*} \right), \tag{A21}$$

we can rewrite Equation (A20) in the equivalent form

$$i\hbar \frac{\partial \psi}{\partial t} = -\frac{\hbar^2}{2m}\Delta \psi + m\Phi \psi + V\psi + \hbar\gamma_I \ln |\psi| \psi - i\frac{\hbar}{2}\gamma_R \ln \left(\frac{\psi}{\psi^*} \right) \psi. \tag{A22}$$

Introducing the notations

$$\gamma_R = \xi, \quad \gamma_I = \frac{2k_B T}{\hbar}, \tag{A23}$$

the generalized Schrödinger Equation (A22) becomes

$$i\hbar \frac{\partial \psi}{\partial t} = -\frac{\hbar^2}{2m}\Delta \psi + m\Phi \psi + V\psi + 2k_B T \ln |\psi| \psi - i\frac{\hbar}{2}\xi \ln \left(\frac{\psi}{\psi^*} \right) \psi. \tag{A24}$$

As shown in [71] (see also Section 2.2), ξ plays the role of an ordinary friction coefficient while T plays the role of an effective temperature. Since the temperature is effective, it can be positive or

negative. Finally, we choose the function $V(t)$ so that the average value of the friction term proportional to ξ is equal to zero. This gives

$$V(t) = i\frac{\hbar}{2}\xi \left\langle \ln \left(\frac{\psi}{\psi^*} \right) \right\rangle, \tag{A25}$$

where $\langle X \rangle = \int \rho X dx$. Then, the generalized Schrödinger Equation (A24) takes the form [71]

$$i\hbar \frac{\partial \psi}{\partial t} = -\frac{\hbar^2}{2m} \Delta \psi + m\Phi \psi + 2k_B T \ln |\psi| \psi - i\frac{\hbar}{2}\xi \left[\ln \left(\frac{\psi}{\psi^*} \right) - \left\langle \ln \left(\frac{\psi}{\psi^*} \right) \right\rangle \right] \psi. \tag{A26}$$

This equation is equivalent to the equation of motion (A13). It is interesting to note that the complex nature of the friction coefficient,

$$\gamma = \xi + i\frac{2k_B T}{\hbar}, \tag{A27}$$

leads to a generalized Schrödinger equation exhibiting *simultaneously* a friction term and an effective temperature term. They correspond to the real and imaginary parts of γ . This may be viewed as a new form of fluctuation-dissipation theorem. As a result, the generalized Schrödinger Equation (A26) introduced by Chavanis [71] connects the generalized Schrödinger equation with a friction term introduced by Kostin [88] and the generalized Schrödinger equation with a logarithmic nonlinearity introduced by Bialynicki-Birula and Mycielski [89]. Remarkably, this equation can be obtained from a unique equation of motion, Equation (A13), by using the formalism of scale relativity [63].

Remark A1. Equation (A26) can be interpreted as a generalized Gross–Pitaevskii (GP) equation with a logarithmic nonlinearity and a dissipation term. This is a particular case of the generalized GP equations considered in [61]. General properties of these equations are established in [61].

Appendix C. Derivation of the GPP Equations in an Expanding Universe

In the main text, we have directly written the GPP Equations (7) and (8) in an expanding universe. Following our previous work [58], this can be justified as follows. We start from the KGE equations for a complex SF (see Equations (9) and (16) of [58]) and use the conformal Newtonian gauge (see Equation (17) of [58]) which is a perturbed form of the Friedmann–Lemaître–Robertson–Walker (FLRW) metric taking into account the expansion of the Universe. We then make the Klein transformation (see Equation (34) of [58]) and finally take the nonrelativistic limit $c \rightarrow +\infty$ to obtain the GPP equations in an expanding background.¹⁹ In this Appendix, we propose an alternative derivation. We start from the nonrelativistic GPP equations in the inertial frame, show that they admit a time-dependent spatially homogeneous solution (describing an expanding universe in a Newtonian cosmology), and finally transform the GPP equations in the comoving frame.

Appendix C.1. Inertial Frame

In the inertial frame, the GPP equations write

$$i\hbar \frac{\partial \psi}{\partial t} = -\frac{\hbar^2}{2m} \Delta \psi + m \frac{dV}{d|\psi|^2} \psi + m\Phi \psi - i\frac{\hbar}{2}\xi \left[\ln \left(\frac{\psi}{\psi^*} \right) - \left\langle \ln \left(\frac{\psi}{\psi^*} \right) \right\rangle \right] \psi - \frac{1}{2}\xi m H (r^2 - \langle r^2 \rangle) \psi, \tag{A28}$$

$$\Delta \Phi = 4\pi G |\psi|^2. \tag{A29}$$

¹⁹ A similar derivation can be performed for a real SF as shown in Sec. II of [90] and in Appendix A of [26].

The last term in Equation (A28) comes from the fact that the friction force manifests itself only in the deviation from the expanding background (see footnote 7). Writing the wave function as

$$\psi(\mathbf{r}, t) = \sqrt{\rho(\mathbf{r}, t)} e^{iS(\mathbf{r}, t)/\hbar}, \tag{A30}$$

where $\rho(\mathbf{r}, t)$ is the mass density and $S(\mathbf{r}, t)$ is the action, and making the Madelung [68] transformation

$$\rho(\mathbf{r}, t) = |\psi|^2 \quad \text{and} \quad \mathbf{u} = \frac{\nabla S}{m}, \tag{A31}$$

where $\mathbf{u}(\mathbf{r}, t)$ is the velocity field, we obtain the hydrodynamic equations in the inertial frame

$$\frac{\partial \rho}{\partial t} + \nabla \cdot (\rho \mathbf{u}) = 0, \tag{A32}$$

$$\frac{\partial S}{\partial t} + \frac{(\nabla S)^2}{2m} = -Q - m\Phi - mV'(\rho) - \zeta(S - \langle S \rangle) + \frac{1}{2} \zeta m H (r^2 - \langle r^2 \rangle), \tag{A33}$$

$$\frac{\partial \mathbf{u}}{\partial t} + (\mathbf{u} \cdot \nabla) \mathbf{u} = -\frac{1}{\rho} \nabla P - \nabla \Phi - \frac{1}{m} \nabla Q - \zeta(\mathbf{u} - H\mathbf{r}), \tag{A34}$$

$$\Delta \Phi = 4\pi G \rho, \tag{A35}$$

where

$$Q = -\frac{\hbar^2}{2m} \frac{\Delta \sqrt{\rho}}{\sqrt{\rho}} = -\frac{\hbar^2}{4m} \left[\frac{\Delta \rho}{\rho} - \frac{1}{2} \frac{(\nabla \rho)^2}{\rho^2} \right] \tag{A36}$$

is the quantum potential taking into account the Heisenberg uncertainty principle, and P is the pressure determined by Equation (19). In line with the remark made after Equation (A29), we see on Equation (A34) that the friction force manifests itself only when the fluid velocity \mathbf{u} deviates from the Hubble flow $H\mathbf{r}$. In the strong friction limit $\zeta \rightarrow +\infty$, the fluid velocity is given at leading order by $\mathbf{u} \simeq H\mathbf{r}$. Then, at next order, the quantum Euler Equation (A34) becomes

$$(\dot{H} + H^2)\mathbf{r} = -\frac{1}{\rho} \nabla P - \nabla \Phi - \frac{1}{m} \nabla Q - \zeta(\mathbf{u} - H\mathbf{r}). \tag{A37}$$

Combining this relation with the continuity Equation (A32), we obtain the quantum Smoluchowski equation in the inertial frame

$$\frac{\partial \rho}{\partial t} + \nabla \cdot (\rho H\mathbf{r}) = \frac{1}{\zeta} \nabla \cdot \left[\nabla P + \rho \nabla \Phi + \frac{\rho}{m} \nabla Q + \rho (\dot{H} + H^2)\mathbf{r} \right]. \tag{A38}$$

Appendix C.2. Newtonian Cosmology

We now derive the basic equations of Newtonian cosmology. We consider a spatially homogeneous solution of Equations (A32)–(A35) of the form

$$\rho_b(\mathbf{r}, t) = \rho_b(t), \quad S_b(\mathbf{r}, t) = \frac{1}{2} H(t) m r^2 + S_0(t), \quad \mathbf{u}_b(\mathbf{r}, t) = H(t)\mathbf{r}, \quad \Phi_b(\mathbf{r}, t) = \frac{2}{3} \pi G \rho_b(t) r^2, \tag{A39}$$

where $H = \dot{a}/a$ is the Hubble constant (actually a function of time) and $a(t)$ is the scale factor. The velocity is assumed to be proportional to the distance (Hubble’s law) and the gravitational potential has been determined from the Poisson equation $\Delta \Phi_b = 4\pi G \rho_b$. The corresponding wavefunction is

$$\psi_b(\mathbf{r}, t) = \sqrt{\rho_b(t)} e^{i[\frac{1}{2} H(t) m r^2 + S_0(t)]/\hbar}. \tag{A40}$$

Under these assumptions, the hydrodynamic Equations (A32)–(A34) reduce to

$$\frac{d\rho_b}{dt} + 3H\rho_b = 0 \quad \Rightarrow \quad \rho_b \propto a^{-3}, \tag{A41}$$

$$\frac{dS_0}{dt} = -mV'(\rho_b), \tag{A42}$$

$$\dot{H} + H^2 = -\frac{4}{3}\pi G\rho_b \quad \Rightarrow \quad \ddot{a} = -\frac{4}{3}\pi G\rho_b a. \tag{A43}$$

The first equation can be interpreted as the conservation of mass

$$M = \frac{4}{3}\pi\rho_b a^3 \quad \Rightarrow \quad \rho_b = \frac{3M}{4\pi a^3} \tag{A44}$$

and the third equation as the Newtonian equation of dynamics

$$\ddot{a} = -\frac{GM}{a^2} = -\frac{\frac{4}{3}\pi G\rho_b a^3}{a^2} \tag{A45}$$

for a particle submitted to a gravitational field $-GM/a^2$ created by a mass M .²⁰ The first integral of motion is

$$\frac{1}{2} \left(\frac{da}{dt} \right)^2 - \frac{GM}{a} = E \quad \Rightarrow \quad \left(\frac{da}{dt} \right)^2 = \frac{2GM}{a} + 2E = \frac{8}{3}\pi G\rho_b a^2 + 2E. \tag{A46}$$

These equations coincide with the Friedmann equations in the nonrelativistic limit (or for pressureless matter). In the context of general relativity, the term $-2E$ represents the curvature of space κ , where $\kappa = -1, 0, +1$ depending whether the Universe is open, critical, or closed. Both inflationary theory and observations of the CMB favor a flat universe ($\kappa = 0$) so we shall take $E = 0$. In that case, Equation (A46) reduces to

$$\left(\frac{da}{dt} \right)^2 = \frac{8}{3}\pi G\rho_b a^2 \quad \Rightarrow \quad H^2 = \frac{8}{3}\pi G\rho_b. \tag{A47}$$

Together with Equation (A41) this leads to the Einstein–de Sitter (EdS) universe²¹

$$a \propto t^{2/3}, \quad H = \frac{\dot{a}}{a} = \frac{2}{3t}, \quad \rho_b = \frac{1}{6\pi Gt^2}. \tag{A48}$$

Appendix C.3. Comoving Frame

In the comoving frame, we make the change of variables

$$\mathbf{r} = a(t)\mathbf{x}, \quad \psi(\mathbf{r}, t) = \Psi(\mathbf{x}, t)e^{i\frac{1}{2}mHr^2/\hbar}, \tag{A49}$$

where \mathbf{r} is the proper distance. Equation (A49) is a change of variables from proper locally Minkowski coordinates \mathbf{r} to expanding coordinates \mathbf{x} comoving in the background model [77]. The density is given by $\rho = |\Psi|^2$. Defining the gravitational potential $\phi(\mathbf{x}, t)$ by

$$\Phi(\mathbf{r}, t) = \Phi_b(\mathbf{r}, t) + \phi(\mathbf{x}, t), \tag{A50}$$

²⁰ These equations can be justified in a Newtonian cosmology if we view the Universe as a homogeneous sphere of mass M , radius $a(t)$ and density $\rho_b(t)$ evolving under its own gravitation. Equation (A45) is then obtained by considering the force experienced by a particle of arbitrary mass m on the surface of this sphere and using Newton’s law.

²¹ Throughout the paper we have assumed a vanishing cosmological constant ($\Lambda = 0$).

we find that the Poisson Equation (A35) becomes

$$\Delta\phi = 4\pi Ga^2(\rho - \rho_b), \tag{A51}$$

where the derivatives are with respect to \mathbf{x} (the same is true for the following equations unless explicitly specified).

We now transform the generalized GPP Equations (A28) and (A29) to the comoving frame. We first compute

$$\begin{aligned} \left(\frac{\partial\psi}{\partial t}\right)_{\mathbf{r}} &= \left(\frac{\partial}{\partial t}\right)_{\mathbf{r}} \Psi\left(\frac{\mathbf{r}}{a(t)}, t\right) e^{i\frac{1}{2}mHr^2/\hbar} \\ &= \left(\frac{\partial\Psi}{\partial t} - H\mathbf{x} \cdot \nabla\Psi + \frac{i}{2\hbar}m\dot{H}a^2x^2\Psi\right) e^{i\frac{1}{2}mHr^2/\hbar}, \end{aligned} \tag{A52}$$

$$\Delta_{\mathbf{r}}\psi = \left(\frac{1}{a^2}\Delta\Psi + 3\frac{i}{\hbar}mH\Psi + 2\frac{i}{\hbar}mH\mathbf{x} \cdot \nabla\Psi - \frac{m^2H^2}{\hbar^2}a^2x^2\Psi\right) e^{i\frac{1}{2}mHr^2/\hbar}, \tag{A53}$$

and

$$-i\frac{\hbar}{2}\xi \ln\left(\frac{\psi}{\psi^*}\right) \psi = \left[-i\frac{\hbar}{2}\xi \ln\left(\frac{\Psi}{\Psi^*}\right) + \frac{1}{2}\xi mHa^2x^2\right] \Psi e^{i\frac{1}{2}mHr^2/\hbar}. \tag{A54}$$

Substituting the foregoing relations into Equation (A28) we find after simplification (using Equation (A43)) that

$$i\hbar\frac{\partial\Psi}{\partial t} + \frac{3}{2}i\hbar H\Psi = -\frac{\hbar^2}{2ma^2}\Delta\Psi + m\frac{dV}{d|\Psi|^2}\Psi + m\phi\Psi - i\frac{\hbar}{2}\xi \left[\ln\left(\frac{\Psi}{\Psi^*}\right) - \left\langle \ln\left(\frac{\Psi}{\Psi^*}\right) \right\rangle\right] \Psi. \tag{A55}$$

On the other hand, using Equation (A47), the Poisson Equation (A51) can be written as

$$\frac{\Delta\phi}{4\pi Ga^2} = |\Psi|^2 - \frac{3H^2}{8\pi G}. \tag{A56}$$

We now proceed in transforming the hydrodynamic Equations (A32)–(A34) to the comoving frame. The wave function can be written as

$$\Psi(\mathbf{x}, t) = \sqrt{\rho(\mathbf{x}, t)} e^{iS(\mathbf{x}, t)/\hbar}, \tag{A57}$$

where $\rho(\mathbf{x}, t)$ is the mass density and $S(\mathbf{x}, t)$ is the action in the comoving frame. Making the Madelung [68] transformation

$$\rho(\mathbf{x}, t) = |\Psi|^2 \quad \text{and} \quad \mathbf{v} = \frac{\nabla S}{ma}, \tag{A58}$$

where $\mathbf{v}(\mathbf{x}, t)$ is the velocity field in the comoving frame, and comparing Equations (A30), (A49) and (A57), we get

$$S(\mathbf{r}, t) = S(\mathbf{x}, t) + \frac{1}{2}mHr^2 \quad \Rightarrow \quad \mathbf{u}(\mathbf{r}, t) = \mathbf{v}(\mathbf{x}, t) + H\mathbf{r}, \tag{A59}$$

where \mathbf{u} is the velocity field in the inertial frame and $H\mathbf{r}$ is the Hubble flow.²² Then, we compute

$$\left(\frac{\partial \rho}{\partial t}\right)_{\mathbf{r}} = \left(\frac{\partial}{\partial t}\right)_{\mathbf{r}} \rho\left(\frac{\mathbf{r}}{a(t)}, t\right) = \frac{\partial \rho}{\partial t} - H\mathbf{x} \cdot \nabla \rho \tag{A60}$$

and

$$\nabla_{\mathbf{r}}(\rho \mathbf{u}) = \frac{1}{a} \nabla \cdot (\rho \mathbf{v}) + H\mathbf{x} \cdot \nabla \rho + 3H\rho. \tag{A61}$$

With these relations, the continuity Equation (A32) becomes

$$\frac{\partial \rho}{\partial t} + 3H\rho + \frac{1}{a} \nabla \cdot (\rho \mathbf{v}) = 0. \tag{A62}$$

Similarly, using

$$\left(\frac{\partial \mathbf{u}}{\partial t}\right)_{\mathbf{r}} = \left(\frac{\partial}{\partial t}\right)_{\mathbf{r}} \mathbf{v}\left(\frac{\mathbf{r}}{a(t)}, t\right) + \dot{H}\mathbf{r} = \frac{\partial \mathbf{v}}{\partial t} - H(\mathbf{x} \cdot \nabla)\mathbf{v} + \dot{H}a\mathbf{x}, \tag{A63}$$

and

$$(\mathbf{u} \cdot \nabla_{\mathbf{r}})\mathbf{u} = [(H\mathbf{r} + \mathbf{v}) \cdot \nabla_{\mathbf{r}}](H\mathbf{r} + \mathbf{v}) = H^2 a\mathbf{x} + H(\mathbf{x} \cdot \nabla)\mathbf{v} + H\mathbf{v} + \frac{1}{a}(\mathbf{v} \cdot \nabla)\mathbf{v}, \tag{A64}$$

the quantum Euler Equation (A34) becomes

$$\frac{\partial \mathbf{v}}{\partial t} + \frac{1}{a}(\mathbf{v} \cdot \nabla)\mathbf{v} + H\mathbf{v} = -\frac{1}{\rho a} \nabla P - \frac{1}{a} \nabla \phi - \frac{1}{ma} \nabla Q - \zeta \mathbf{v} \tag{A65}$$

with the quantum potential

$$Q = -\frac{\hbar^2}{2ma^2} \frac{\Delta \sqrt{\rho}}{\sqrt{\rho}} = -\frac{\hbar^2}{4ma^2} \left[\frac{\Delta \rho}{\rho} - \frac{1}{2} \frac{(\nabla \rho)^2}{\rho^2} \right], \tag{A66}$$

where we have used Equation (A43) to simplify some terms. These transformations can also be made at the level of the action. Using

$$\left(\frac{\partial S}{\partial t}\right)_{\mathbf{r}} = \left(\frac{\partial}{\partial t}\right)_{\mathbf{r}} S\left(\frac{\mathbf{r}}{a(t)}, t\right) + \frac{1}{2} m \dot{H} r^2 = \frac{\partial S}{\partial t} - H\mathbf{x} \cdot \nabla S + \frac{1}{2} m \dot{H} r^2 \tag{A67}$$

and

$$\nabla_{\mathbf{r}} S = \frac{1}{a} \nabla S + m H \mathbf{r}, \tag{A68}$$

the quantum Hamilton–Jacobi Equation (A33) becomes after simplification

$$\frac{\partial S}{\partial t} + \frac{(\nabla S)^2}{2ma^2} = -Q - m\phi - mV'(\rho) - \zeta(S - \langle S \rangle). \tag{A69}$$

Finally, we transform the Smoluchowski Equation (A38) to the comoving frame. Using Equations (A39), (A43), (A50) and (A60), we get

$$\frac{\partial \rho}{\partial t} + 3H\rho = \frac{1}{\zeta a^2} \nabla \cdot \left(\nabla P + \rho \nabla \phi + \frac{\rho}{m} \nabla Q \right). \tag{A70}$$

²² This result can also be obtained as follows. Taking the derivative with respect to time of the relation $\mathbf{r} = a(t)\mathbf{x}$, we get $d\mathbf{r}/dt = \dot{a}\mathbf{x} + a d\mathbf{x}/dt$. This can be written as $\mathbf{u} = H\mathbf{r} + \mathbf{v}$ with $\mathbf{u} = d\mathbf{r}/dt$ and $\mathbf{v} = a d\mathbf{x}/dt$, where \mathbf{u} is the proper velocity and \mathbf{v} is the peculiar velocity.

We can check that the above results return the equations of Sections 2.1 and 2.2 up to an obvious change of notations.

Appendix D. Gravitational Bogoliubov Equations

In this Appendix, following Ref. [67], we derive the quantum Jeans dispersion relation from the gravitational Bogoliubov equations for quasi-particle excitations. We directly work on the GPP equations without introducing the hydrodynamic variables.

The GPP equations can be written as

$$i\hbar \frac{\partial \psi}{\partial t} = -\frac{\hbar^2}{2m} \Delta \psi + m \frac{dV}{d|\psi|^2} \psi + m\Phi \psi + m\Phi_{\text{ext}} \psi, \tag{A71}$$

$$\Phi(\mathbf{r}, t) = \int u_G(|\mathbf{r} - \mathbf{r}'|) |\psi|^2(\mathbf{r}', t) d\mathbf{r}', \tag{A72}$$

where $u_G(|\mathbf{r} - \mathbf{r}'|) = -G/|\mathbf{r} - \mathbf{r}'|$ denotes the gravitational potential of interaction. A stationary solution of the GPP equations is of the form

$$\psi_0(\mathbf{r}, t) = \psi_0(\mathbf{r}) e^{-iE_0 t/\hbar}, \tag{A73}$$

where the real quantities $\psi_0(\mathbf{r}) = \sqrt{\rho_0(\mathbf{r})}$ and E_0 are determined by the eigenvalue equation

$$-\frac{\hbar^2}{2m} \Delta \psi_0 + mV'(|\psi_0|^2) \psi_0 + m\Phi_0 \psi_0 + m\Phi_{\text{ext}} \psi_0 = E_0 \psi_0 \tag{A74}$$

with

$$\Phi_0(\mathbf{r}) = \int u_G(|\mathbf{r} - \mathbf{r}'|) |\psi_0|^2(\mathbf{r}') d\mathbf{r}'. \tag{A75}$$

We now consider a small perturbation about this stationary solution and write the wavefunction as

$$\psi(\mathbf{r}, t) = e^{-iE_0 t/\hbar} [\psi_0(\mathbf{r}) + \delta\psi(\mathbf{r}, t)] \tag{A76}$$

with $|\delta\psi| \ll \psi_0$. The density is given at linear order by

$$\rho = |\psi|^2 = (\psi_0 + \delta\psi)(\psi_0^* + \delta\psi^*) \simeq |\psi_0|^2 + \psi_0 \delta\psi^* + \psi_0^* \delta\psi. \tag{A77}$$

Therefore, we have

$$\rho_0 = |\psi_0|^2 \quad \text{and} \quad \delta\rho = \psi_0 \delta\psi^* + \psi_0^* \delta\psi. \tag{A78}$$

Substituting these relations into the GP Equation (A71), we obtain at linear order

$$i\hbar \frac{\partial \delta\psi}{\partial t} = \left[-\frac{\hbar^2}{2m} \Delta + mV'(|\psi_0|^2) + mV''(|\psi_0|^2) |\psi_0|^2 + m\Phi_0 + m\Phi_{\text{ext}} - E_0 \right] \delta\psi + m\delta\Phi \psi_0 + mV''(|\psi_0|^2) \psi_0^2 \delta\psi^*. \tag{A79}$$

The gravitational potential defined by Equation (A72) can be written as

$$\Phi = u_G * \rho = u_G * |\psi|^2, \tag{A80}$$

where $*$ denotes the product of convolution. According to Equation (A78), we have

$$\Phi_0 = u_G * \rho_0 = u_G * |\psi_0|^2 \quad \text{and} \quad \delta\Phi = u_G * \delta\rho = u_G * (\psi_0 \delta\psi^* + \psi_0^* \delta\psi). \tag{A81}$$

Substituting Equation (A81) into Equation (A79), we find that the equation of motion for $\delta\psi(\mathbf{r}, t)$ is

$$i\hbar \frac{\partial \delta\psi}{\partial t} = \left[-\frac{\hbar^2}{2m} \Delta + mV'(|\psi_0|^2) + mV''(|\psi_0|^2)|\psi_0|^2 + mu_G * |\psi_0|^2 + m\Phi_{\text{ext}} - E_0 \right] \delta\psi + m [u_G * (\psi_0 \delta\psi^* + \psi_0^* \delta\psi)] \psi_0 + mV''(|\psi_0|^2) \psi_0^2 \delta\psi^*. \tag{A82}$$

We obtain a similar equation of motion for the complex conjugate $\delta\psi(\mathbf{r}, t)^*$. Solving these two equations with the ansatz

$$\delta\psi(\mathbf{r}, t) = u(\mathbf{r})e^{-i\omega t} - v^*(\mathbf{r})e^{i\omega t}, \tag{A83}$$

we obtain the following pair of coupled equations for $u(\mathbf{r})$ and $v(\mathbf{r})$:

$$\hbar\omega u = \left[-\frac{\hbar^2}{2m} \Delta + mV'(|\psi_0|^2) + mV''(|\psi_0|^2)|\psi_0|^2 + mu_G * |\psi_0|^2 + m\Phi_{\text{ext}} - E_0 \right] u + m [u_G * (-\psi_0 v + \psi_0^* u)] \psi_0 - mV''(|\psi_0|^2) \psi_0^2 v, \tag{A84}$$

$$\hbar\omega v = - \left[-\frac{\hbar^2}{2m} \Delta + mV'(|\psi_0|^2) + mV''(|\psi_0|^2)|\psi_0|^2 + mu_G * |\psi_0|^2 + m\Phi_{\text{ext}} - E_0 \right] v + m [u_G * (\psi_0^* u - \psi_0 v)] \psi_0^* + mV''(|\psi_0|^2) (\psi_0^*)^2 u, \tag{A85}$$

which will be referred to as the gravitational Bogoliubov equations. Regrouping the terms in u and v , they can be rewritten more symmetrically as

$$\left[-\frac{\hbar^2}{2m} \Delta + mV'(|\psi_0|^2) + mV''(|\psi_0|^2)|\psi_0|^2 + mu_G * |\psi_0|^2 + m\Phi_{\text{ext}} - E_0 - \hbar\omega \right] u + m [u_G * (\psi_0^* u)] \psi_0 = mV''(|\psi_0|^2) \psi_0^2 v + m [u_G * (\psi_0 v)] \psi_0, \tag{A86}$$

$$\left[-\frac{\hbar^2}{2m} \Delta + mV'(|\psi_0|^2) + mV''(|\psi_0|^2)|\psi_0|^2 + mu_G * |\psi_0|^2 + m\Phi_{\text{ext}} - E_0 + \hbar\omega \right] v + m [u_G * (\psi_0 v)] \psi_0^* = mV''(|\psi_0|^2) (\psi_0^*)^2 u + m [u_G * (\psi_0^* u)] \psi_0^*. \tag{A87}$$

For the nongravitational standard BEC, we recover the usual Bogoliubov equations

$$\left[-\frac{\hbar^2}{2m} \Delta + 2mg|\psi_0|^2 + m\Phi_{\text{ext}} - E_0 - \hbar\omega \right] u = mg\psi_0^2 v, \tag{A88}$$

$$\left[-\frac{\hbar^2}{2m} \Delta + 2mg|\psi_0|^2 + m\Phi_{\text{ext}} - E_0 + \hbar\omega \right] v = mg(\psi_0^*)^2 u, \tag{A89}$$

with $g = 4\pi a_s \hbar^2 / m^3$. We now come back to the GPP Equations (A71) and (A72) and take $\Phi_{\text{ext}} = 0$. For a spatially homogeneous equilibrium state, for which $\psi_0(t) = \psi_0$, the eigenenergy E_0 is given by [see Equation (A74)]²³

$$E_0 = mV'(|\psi_0|^2) + mu_G * |\psi_0|^2, \tag{A90}$$

²³ The gravitational potential must be modified as explained in footnote 12 to avoid the Jeans swindle.

and the gravitational Bogoliubov Equations (A86) and (A87) reduce to

$$\left[-\frac{\hbar^2}{2m}\Delta + mV''(\rho)\rho - \hbar\omega \right] u + m(u_G * u)\rho = mV''(\rho)\rho v + m(u_G * v)\rho, \tag{A91}$$

$$\left[-\frac{\hbar^2}{2m}\Delta + mV''(\rho)\rho + \hbar\omega \right] v + m(u_G * v)\rho = mV''(\rho)\rho u + m(u_G * u)\rho, \tag{A92}$$

where we have denoted the equilibrium density by ρ instead of ρ_0 . Considering plane-wave solutions of the form

$$u(\mathbf{r}) = ue^{i\mathbf{k}\cdot\mathbf{r}} \quad \text{and} \quad v(\mathbf{r}) = ve^{i\mathbf{k}\cdot\mathbf{r}}, \tag{A93}$$

the foregoing equations become

$$\left[\frac{\hbar^2 k^2}{2m} + mV''(\rho)\rho - \hbar\omega + m\rho(2\pi)^3 \hat{u}_G(k) \right] u - \left[mV''(\rho)\rho + m\rho(2\pi)^3 \hat{u}_G(k) \right] v = 0, \tag{A94}$$

$$\left[\frac{\hbar^2 k^2}{2m} + mV''(\rho)\rho + \hbar\omega + m\rho(2\pi)^3 \hat{u}_G(k) \right] v - \left[mV''(\rho)\rho + m\rho(2\pi)^3 \hat{u}_G(k) \right] u = 0. \tag{A95}$$

These two equations are consistent only if the determinant of the coefficients vanishes. This leads after simplification to the condition

$$\omega^2 = \frac{\hbar^2 k^4}{4m^2} + V''(\rho)\rho k^2 + \rho(2\pi)^3 \hat{u}_G(k)k^2. \tag{A96}$$

Recalling the identity from Equation (20), and introducing explicitly the Fourier transform of the gravitational potential given by

$$(2\pi)^3 \hat{u}_G(k) = -\frac{4\pi G}{k^2}, \tag{A97}$$

we obtain the quantum Jeans dispersion relation

$$\omega^2 = \frac{\hbar^2 k^4}{4m^2} + c_s^2 k^2 - 4\pi G\rho. \tag{A98}$$

References

1. Ade, P.A.R. [Planck Collaboration] Planck 2015 results. XIII. Cosmological parameters. *Astron. Astrophys.* **2016**, *594*, A13.
2. Einstein, A. Kosmologische Betrachtungen zur allgemeinen Relativitäts theorie. *Sitzungsber. Preuss. Akad. Wiss.* **1917**, *1*, 142.
3. Caldwell, R.R.; Dave, R.; Steinhardt, P.J. Cosmological Imprint of an Energy Component with General Equation of State. *Phys. Rev. Lett.* **1998**, *80*, 1582. [[CrossRef](#)]
4. Kamenshchik, A.; Moschella, U.; Pasquier, V. An alternative to quintessence. *Phys. Lett. B* **2001**, *511*, 265.
5. Rubin, V.C.; Ford, W.K. Rotation of the Andromeda Nebula from a Spectroscopic Survey of Emission Regions. *Astrophys. J.* **1970**, *159*, 379. [[CrossRef](#)]
6. Zwicky, F. Die Rotverschiebung von extragalaktischen Nebeln. *Helv. Phys. Acta* **1933**, *6*, 110–127.

7. Milgrom, M. A modification of the Newtonian dynamics as a possible alternative to the hidden mass hypothesis. *Astrophys. J.* **1983**, *270*, 365–370. [[CrossRef](#)]
8. Binney, J.; Tremaine, S. *Galactic Dynamics*; Princeton Series in Astrophysics: Princeton, NJ, USA, 1987.
9. Jungman, G.; Kamionkowski, M.; Griest, K. Supersymmetric Dark Matter. *Phys. Rep.* **1996**, *267*, 195. [[CrossRef](#)]
10. Navarro, J.F.; Frenk, C.S.; White, S.D.M. A Universal Density Profile from Hierarchical Clustering. *Astrophys. J.* **1996**, *462*, 563. [[CrossRef](#)]
11. Burkert, A. The Structure of Dark Matter Halos in Dwarf Galaxies. *Astrophys. J.* **1996**, *447*, L25.
12. Moore, B.; Quinn, T.; Governato, F.; Stadel, J.; Lake, G. Cold collapse and the core catastrophe. *Mon. Not. R. Astron. Soc.* **1999**, *310*, 1147–1152. [[CrossRef](#)]
13. Klypin, A.; Kravtsov, A.V.; Valenzuela, O. Where Are the Missing Galactic Satellites? *Astrophys. J.* **1999**, *522*, 82.
14. Boylan-Kolchin, M.; Bullock, J.S.; Kaplinghat, M. Too big to fail? The puzzling darkness of massive Milky Way subhaloes. *Mon. Not. R. Astron. Soc.* **2011**, *415*, L40. [[CrossRef](#)]
15. Bullock, J.S.; Boylan-Kolchin, M. Small-Scale Challenges to the Λ CDM Paradigm. *Ann. Rev. Astron. Astrophys.* **2017**, *55*, 343. [[CrossRef](#)]
16. Romano-Díaz, E.; Shlosman, I.; Hoffman, Y.; Heller, C. Erasing Dark Matter Cusps in Cosmological Galactic Halos with Baryons. *Astrophys. J.* **2008**, *685*, L105. [[CrossRef](#)]
17. Spergel, D.N.; Steinhardt, P.J. Observational Evidence for Self-Interacting Cold Dark Matter. *Phys. Rev. Lett.* **2000**, *84*, 3760. [[CrossRef](#)] [[PubMed](#)]
18. Bode, P.; Ostriker, J.P.; Turok, N. Halo Formation in Warm Dark Matter Models. *Astrophys. J.* **2001**, *556*, 93. [[CrossRef](#)]
19. Chavanis, P.H. Statistical mechanics of self-gravitating systems in general relativity: I. The quantum Fermi gas. *Eur. Phys. J. Plus* **2020**, *135*, 1–79. [[CrossRef](#)]
20. Chandrasekhar, S. *An Introduction to the Study of Stellar Structure*; Dover Publications: Mineola, NY, USA, 1958.
21. Suárez, A.; Chavanis, P.H. Cosmological evolution of a complex scalar field with repulsive or attractive self-interaction. *Phys. Rev. D* **2017**, *95*, 063515. [[CrossRef](#)]
22. Chavanis, P.H. Derivation of the core mass-halo mass relation of fermionic and bosonic dark matter halos from an effective thermodynamical model. *Phys. Rev. D* **2019**, *100*, 123506. [[CrossRef](#)]
23. De Vega, H.J.; Salucci, P.; Sanchez, N.G. Observational rotation curves and density profiles versus the Thomas-Fermi galaxy structure theory. *Mon. Not. R. Astron. Soc.* **2014**, *442*, 2717–2727. [[CrossRef](#)]
24. Ruffini, R.; Argüelles, C.R.; Rueda, J.A. On the core-halo distribution of dark matter in galaxies. *Mon. Not. R. Astron. Soc.* **2015**, *451*, 622. [[CrossRef](#)]
25. Chavanis, P.H.; Lemou, M.; Méhats, F. Models of dark matter halos based on statistical mechanics: The fermionic King model. *Phys. Rev. D* **2015**, *92*, 123527. [[CrossRef](#)]
26. Chavanis, P.H. Quantum tunneling rate of dilute axion stars close to the maximum mass. *Phys. Rev. D* **2020**, *102*, 083531. [[CrossRef](#)]
27. Böhmer, C.G.; Harko, T. Can dark matter be a Bose–Einstein condensate? *J. Cosmol. Astropart. Phys.* **2007**, *6*, 025. [[CrossRef](#)]
28. Chavanis, P.H. Mass-radius relation of Newtonian self-gravitating Bose-Einstein condensates with short-range interactions. I. Analytical results. *Phys. Rev. D* **2011**, *84*, 043531. [[CrossRef](#)]
29. Kaup, D.J. Klein-Gordon Geon. *Phys. Rev.* **1968**, *172*, 1331. [[CrossRef](#)]
30. Ruffini, R.; Bonazzola, S. Systems of Self-Gravitating Particles in General Relativity and the Concept of an Equation of State. *Phys. Rev.* **1969**, *187*, 1767. [[CrossRef](#)]
31. Oppenheimer, J.R.; Volkoff, G.M. On Massive Neutron Cores. *Phys. Rev.* **1939**, *55*, 374. [[CrossRef](#)]
32. Colpi, M.; Shapiro, S.L.; Wasserman, I. Boson Stars: Gravitational Equilibria of Self-Interacting Scalar Fields. *Phys. Rev. Lett.* **1986**, *57*, 2485. [[CrossRef](#)]
33. Chavanis, P.H.; Harko, T. Bose-Einstein condensate general relativistic stars. *Phys. Rev. D* **2012**, *86*, 064011. [[CrossRef](#)]
34. Schive, H.Y.; Chiueh, T.; Broadhurst, T. Cosmic structure as the quantum interference of a coherent dark wave. *Nat. Phys.* **2014**, *10*, 496. [[CrossRef](#)]

35. Schive, H.Y.; Liao, M.H.; Woo, T.P.; Wong, S.K.; Chiueh, T.; Broadhurst, T.; Pauchy Hwang, W.Y. Understanding the Core-Halo Relation of Quantum Wave Dark Matter from 3D Simulations. *Phys. Rev. Lett.* **2014**, *113*, 261302. [[CrossRef](#)] [[PubMed](#)]
36. Schwabe, B.; Niemeyer, J.; Engels, J. Simulations of solitonic core mergers in ultralight axion dark matter cosmologies. *Phys. Rev. D* **2016**, *94*, 043513. [[CrossRef](#)]
37. Mocz, P.; Vogelsberger, M.; Robles, V.H.; Zavala, J.; Boylan-Kolchin, M.; Fialkov, A.; Hernquist, L. Galaxy formation with BECDM—I. Turbulence and relaxation of idealized haloes. *Mon. Not. R. Astron. Soc.* **2017**, *471*, 4559. [[CrossRef](#)]
38. Mocz, P.; Lancaster, L.; Fialkov, A.; Becerra, F.; Chavanis, P.H. Schrödinger-Poisson–Vlasov-Poisson correspondence. *Phys. Rev. D* **2018**, *97*, 083519. [[CrossRef](#)]
39. Veltmaat, J.; Niemeyer, J.C.; Schwabe, B. Formation and structure of ultralight bosonic dark matter halos. *Phys. Rev. D* **2018**, *98*, 043509. [[CrossRef](#)]
40. Mocz, P.; Fialkov, A.; Vogelsberger, M.; Becerra, F.; Amin, M.A.; Bose, S.; Boylan-Kolchin, M.; Chavanis, P.H.; Hernquist, L.; Lancaster, L.; et al. First Star-Forming Structures in Fuzzy Cosmic Filaments. *Phys. Rev. Lett.* **2019**, *123*, 141301. [[CrossRef](#)]
41. Mocz, P.; Fialkov, A.; Vogelsberger, M.; Becerra, F.; Shen, X.; Robles, V.H.; Amin, M.A.; Zavala, J.; Boylan-Kolchin, M.; Bose, S.; et al. Galaxy formation with BECDM – II. Cosmic filaments and first galaxies. *Mon. Not. R. Astron. Soc.* **2020**, *494*, 2027. [[CrossRef](#)]
42. Lynden-Bell, D. Statistical mechanics of violent relaxation in stellar systems. *Mon. Not. R. Astron. Soc.* **1967**, *136*, 101. [[CrossRef](#)]
43. Seidel, E.; Suen, W.M. Formation of solitonic stars through gravitational cooling. *Phys. Rev. Lett.* **1994**, *72*, 2516. [[CrossRef](#)]
44. Chavanis, P.H.; Lemou, M.; Méhats, F. Models of dark matter halos based on statistical mechanics: The classical King model. *Phys. Rev. D* **2015**, *91*, 063531. [[CrossRef](#)]
45. Chavanis, P.H. Predictive model of BEC dark matter halos with a solitonic core and an isothermal atmosphere. *Phys. Rev. D* **2019**, *100*, 083022. [[CrossRef](#)]
46. Jeans, J.I. The stability of a spherical nebula. *Phil. Trans. R. Soc. Lond. A* **1902**, *199*, 1.
47. Chavanis, P.H. Dynamical stability of infinite homogeneous self-gravitating systems and plasmas: Application of the Nyquist method. *Eur. Phys. J. B* **2012**, *85*, 229. [[CrossRef](#)]
48. Khlopov, M.Y.; Malomed, B.A.; Zeldovich, Y.B. Gravitational instability of scalar fields and formation of primordial black holes. *Mon. Not. R. Astron. Soc.* **1985**, *215*, 575. [[CrossRef](#)]
49. Bianchi, M.; Grasso, D.; Ruffini, R. Jeans mass of a cosmological coherent scalar field. *Astron. Astrophys.* **1990**, *231*, 301.
50. Hu, W.; Barkana, R.; Gruzinov, A. Fuzzy Cold Dark Matter: The Wave Properties of Ultralight Particles. *Phys. Rev. Lett.* **2000**, *85*, 1158. [[CrossRef](#)] [[PubMed](#)]
51. Sikivie, P.; Yang, Q. Bose-Einstein Condensation of Dark Matter Axions. *Phys. Rev. Lett.* **2009**, *103*, 111301. [[CrossRef](#)]
52. Suárez, A.; Chavanis, P.H. Jeans-type instability of a complex self-interacting scalar field in general relativity. *Phys. Rev. D* **2018**, *98*, 083529. [[CrossRef](#)]
53. Harko, T. Jeans instability and turbulent gravitational collapse of Bose–Einstein condensate dark matter halos. *Eur. Phys. J. C* **2019**, *79*, 787. [[CrossRef](#)]
54. Lifshitz, E. On the gravitational stability of the expanding universe. *J. Phys.* **1946**, *10*, 116.
55. Bonnor, W.B. Jeans' Formula for Gravitational Instability. *Mon. Not. R. Astron. Soc.* **1957**, *117*, 104. [[CrossRef](#)]
56. Gilbert, I.H. An Integral Equation for the Development of Irregularities in an Expanding Universe. *Astrophys. J.* **1966**, *144*, 233. [[CrossRef](#)]
57. Chavanis, P.H. Growth of perturbations in an expanding universe with Bose-Einstein condensate dark matter. *Astron. Astrophys.* **2012**, *537*, A127. [[CrossRef](#)]
58. Suárez, A.; Chavanis, P.H. Hydrodynamic representation of the Klein-Gordon-Einstein equations in the weak field limit: General formalism and perturbations analysis. *Phys. Rev. D* **2015**, *92*, 023510. [[CrossRef](#)]
59. Suárez, A.; Matos, T. Structure formation with scalar-field dark matter: The fluid approach. *Mon. Not. R. Astron. Soc.* **2011**, *416*, 87–93.

60. Chavanis, P.H.; Matos, T. Covariant theory of Bose-Einstein condensates in curved spacetimes with electromagnetic interactions: The hydrodynamic approach. *Eur. Phys. J. Plus* **2017**, *132*, 30. [[CrossRef](#)]
61. Chavanis, P.H. Dissipative self-gravitating Bose-Einstein condensates with arbitrary nonlinearity as a model of dark matter halos. *Eur. Phys. J. Plus* **2017**, *132*, 248. [[CrossRef](#)]
62. Chavanis, P.H. Derivation of a generalized Schrödinger equation for dark matter halos from the theory of scale relativity. *Phys. Dark Univ.* **2018**, *22*, 80–95. [[CrossRef](#)]
63. Nottale, L. *Scale Relativity and Fractal Space-Time*; Imperial College Press: London, UK, 2011.
64. Suárez, A.; Chavanis, P.H. Hydrodynamic representation of the Klein-Gordon-Einstein equations in the weak field limit. *J. Phys. Conf. Ser.* **2015**, *654*, 012088.
65. Chavanis, P.H. A heuristic wave equation parameterizing BEC dark matter halos with a quantum core and an isothermal atmosphere. **2020**, in preparation.
66. Chavanis, P.H.; Sommeria, J.; Robert, R. Statistical Mechanics of Two-Dimensional Vortices and Collisionless Stellar Systems. *Astrophys. J.* **1996**, *471*, 385. [[CrossRef](#)]
67. Griffin, A.; Nikuni, T.; Zaremba, E. *Bose-Condensed Gases at Finite Temperatures*; Cambridge University Press: Cambridge, UK, 2009.
68. Madelung, E. Quantentheorie in hydrodynamischer Form. *Z. Phys.* **1927**, *40*, 322. [[CrossRef](#)]
69. Chavanis, P.H. Instability of a uniformly collapsing cloud of classical and quantum self-gravitating Brownian particles. *Phys. Rev. E* **2011**, *84*, 031101. [[CrossRef](#)] [[PubMed](#)]
70. Chavanis, P.H.; Rosier, C.; Sire, C. Thermodynamics of self-gravitating systems. *Phys. Rev. E* **2002**, *66*, 036105. [[CrossRef](#)]
71. Chavanis, P.H. Derivation of a generalized Schrödinger equation from the theory of scale relativity. *Eur. Phys. J. Plus* **2017**, *132*, 286. [[CrossRef](#)]
72. Chavanis, P.H.; Delfini, L. Mass-radius relation of Newtonian self-gravitating Bose-Einstein condensates with short-range interactions. II. Numerical results. *Phys. Rev. D* **2011**, *84*, 043532. [[CrossRef](#)]
73. Kiessling, M. The “Jeans swindle”: A true story—mathematically speaking. *Adv. Appl. Math.* **2003**, *31*, 132. [[CrossRef](#)]
74. Joyce, M. Infinite self-gravitating systems and cosmological structure formation. In *Dynamics and Thermodynamics of Systems with Long Range Interactions: Theory and Experiments*; Campa, A., Giansanti, A., Morigi, G., Labini, F.S., Eds.; American Institute of Physics (AIP): Melville, NY, USA, 2008; Volume 970, p. 237.
75. Joyce, M.; Marcos, B.; Labini, F.S. Dynamics of finite and infinite self-gravitating systems with cold quasi-uniform initial conditions. *J. Stat. Mech.* **2009**, *4*, 04019. [[CrossRef](#)]
76. Chavanis, P.H. Gravitational instability of finite isothermal spheres. *Astron. Astrophys.* **2002**, *381*, 340. [[CrossRef](#)]
77. Peebles, P.J.E. *The Large-Scale Structure of the Universe*; Princeton University Press: Princeton, NJ, USA, 1980.
78. Friedmann, A. Über die Krümmung des Raumes. *Zeits. f. Physik* **1922**, *10*, 377–386.
79. Friedmann, A. Über die Möglichkeit einer Welt mit konstanter negativer Krümmung des Raumes. *Zeits. f. Physik* **1924**, *21*, 326–332. [[CrossRef](#)]
80. Einstein, A.; de Sitter, W. On the Relation between the Expansion and the Mean Density of the Universe. *Proc. Natl. Acad. Sci. USA* **1932**, *18*, 213. [[CrossRef](#)] [[PubMed](#)]
81. Pethick, C.J.; Smith, H. *Bose-Einstein Condensation in Dilute Gases*; Cambridge University Press: Cambridge, UK, 2002.
82. Bogoliubov, N. On the theory of superfluidity. *Phys. J.* **1947**, *11*, 23.
83. Guth, A.H.; Hertzberg, M.P.; Prescod-Weinstein, C. Do dark matter axions form a condensate with long-range correlation? *Phys. Rev. D* **2015**, *92*, 103513. [[CrossRef](#)]
84. Kolb, E.W.; Tkachev, I.I. Nonlinear axion dynamics and the formation of cosmological pseudosolitons. *Phys. Rev. D* **1994**, *49*, 5040. [[CrossRef](#)]
85. Chavanis, P.H.; Sire, C. Jeans type analysis of chemotactic collapse. *Phys. A* **2008**, *387*, 4033. [[CrossRef](#)]
86. Keller, E.F.; Segel, L.A. Model for Chemotaxis. *J. Theor. Biol.* **1971**, *30*, 225. [[CrossRef](#)]
87. Nelson, E. Derivation of the Schrödinger Equation from Newtonian Mechanics. *Phys. Rev.* **1966**, *150*, 1079. [[CrossRef](#)]
88. Kostin, M.D. On the Schrödinger—Langevin Equation. *J. Chem. Phys.* **1972**, *57*, 3589. [[CrossRef](#)]

89. Bialynicki-Birula, I.; Mycielski, J. Nonlinear wave mechanics. *Ann. Phys.* **1976**, *100*, 62. [[CrossRef](#)]
90. Chavanis, P.H. Phase transitions between dilute and dense axion stars. *Phys. Rev. D* **2018**, *98*, 023009. [[CrossRef](#)]

Publisher's Note: MDPI stays neutral with regard to jurisdictional claims in published maps and institutional affiliations.



© 2020 by the author. Licensee MDPI, Basel, Switzerland. This article is an open access article distributed under the terms and conditions of the Creative Commons Attribution (CC BY) license (<http://creativecommons.org/licenses/by/4.0/>).